Quaternary Science Reviews 270 (2021) 107148

Contents lists available at ScienceDirect

Quaternary Science Reviews

journal homepage: www.elsevier.com/locate/quascirev

Modern relationships between microscopic charcoal in marine sediments and fire regimes on adjacent landmasses to refine the interpretation of marine paleofire records: An Iberian case study

Marion Genet [a, *], Anne-Laure Daniau [a], Florent Mouillot [b], Vincent Hanquiez [a], Sabine Schmidt [a], Valérie David [a], Muriel Georget [a], Fatima Abrantes [c, d], Pierre Anschutz [a], Franck Bassinot [e], Jérome Bonnin [a], Bernard Dennielou [f], Frédérique Eynaud [a], David A. Hodell [g], Thierry Mulder [a], Filipa Naughton [c, d], Linda Rossignol [a], Polychronis Tzedakis [h], Maria Fernanda Sánchez-Goñi [a, i]

[a] Univ. Bordeaux, CNRS, EPOC, EPHE, UMR 5805, F-33615 Pessac, France
[b] UMR CEFE, Univ. Montpellier, CNRS, EPHE, IRD, Univ. Paul Valery Montpellier 3, 1919 route de Mende,34293, Montpellier, CEDEX 5, France
[c] Divisão de Geologia e Georecursos Marinhos, Instituto Português do Mar e da Atmosfera (IPMA), Avenida de Brasília 6, Lisboa, 1449-006, Portugal
[d] CCMAR, Centro de Ciências do Mar, Universidade do Algarve, Campus de Gambelas, Faro, 8005-139, Portugal
[e] Laboratoire des Sciences du Climat et de l'Environnement, LSCE/IPSL, CEA-CNRS-UVSQ, Université Paris-Saclay, 91191, Gif-sur-Yvette, France
[f] Ifremer, Unité Géosciences Marines, Centre Bretagne - 29280, Plouzané, France
[g] University of Cambridge, Godwin Laboratory for Palaeoclimate Research, Cambridge, United Kingdom
[h] Environmental Change Research Centre, Department of Geography, University College London, London, WC1E 6BT, United Kingdom
[i] Ecole Pratique des Hautes Etudes (EPHE, PSL University), F-33615, Pessac, France

ARTICLE INFO

Article history:
Received 17 May 2021
Received in revised form
29 July 2021
Accepted 12 August 2021
Available online 30 August 2021

Handling Editor: Giovanni Zanchetta

Keywords:
Microcharcoal
Marine surface sediments
Calibration
Iberian peninsula
Western europe
Fire regime
Climate
Vegetation
Holocene

ABSTRACT

Marine microcharcoal records provide invaluable information to understand changes in biomass burning and its drivers over multiple glacial and interglacial cycles and to evaluate fire models under warmer climates than today. However, quantitative reconstructions of burnt area, fire intensity and frequency from these records need calibration studies of the current fire-microcharcoal relationship. Here, we present the analysis of microcharcoal concentration and morphology in 102 core-top sediment samples collected in the Iberian margin and the Gulf of Cádiz. We show that microcharcoal concentrations are influenced by the water depth or the distance from the river mouth. At regional scale, the mean microcharcoal concentrations and microcharcoal elongation (length to width ratio) show a marked latitudinal variation in their distribution, primarily controlled by the type of burnt vegetation in the adjacent continent. High microcharcoal concentrations in marine sediments represent rare, large and intense fires in open Mediterranean woodlands. Based on these results, the increasing trend of microcharcoal concentrations recorded since 8 ka in the well-known marine sedimentary core MD95-2042 off the Iberian margin indicates the occurrence of large and infrequent fires of high intensity due to the progressive degradation of the Mediterranean forest and the expansion of shrublands.

1. Introduction

Major economic cost is attributed today to wildfire management, fire damage losses and human health problems due to fire emissions (Bowman et al., 2009; Hall, 2014; Lohman et al., 2007; Robinne et al., 2018; Sanchez, 2007). Projected future warmer and drier climate scenarios suggest that these risks and costs are going to increase substantially in certain regions (Liu et al., 2010; Pechony and Shindell, 2010; Settele et al., 2015), in particular in the Mediterranean region (Mouillot et al., 2002; Ruffault et al., 2020). The most important changes in fire risk are linked to the lengthening of the fire season (Moriondo et al., 2006) and to more frequent heat-

* Corresponding author.
E-mail address: marion.genet@u-bordeaux.fr (M. Genet).

https://doi.org/10.1016/j.quascirev.2021.107148

induced fire weather (Ruffault et al., 2020) leading to increased frequency of extreme fire events. However, potential changes in the interactions between climate, vegetation and fire are neglected by these models which are based on modern-day statistical relationships. Fire modules embedded in dynamic vegetation models aim at coupling these interactions and feedbacks (Hantson et al., 2016). These process-based models must be tested, not only with modern observations based on global remote sensing (Mouillot et al., 2014) or recent fire history (Mouillot et al., 2005), but also with observations from climate conditions different from today and especially similar to the range of climate variability projected for the next centuries (Hantson et al., 2016).

Terrestrial and marine sedimentary charcoal records provide invaluable information about the past fire regime variability. Charcoal is a carbonaceous material mostly composed of pure carbon formed at temperature between 200 and 600 °C (Conedera et al., 2009) by pyrolysis during the combustion process of vegetation. When extracted from sedimentary records, it can be used to examine past fire regime variability. Charcoal is classified as inertinite, being relatively resistant to chemical and microbial decomposition (Habib et al., 1994; Hart et al., 1994; Hockaday et al., 2006; Quénéa et al., 2006; Verardo, 1997), especially if burial occurs in depositional environments with high sedimentation rates. While few charcoal terrestrial records (lake, mire, bog) go back to the last glacial period (Daniau et al., 2010), marine sedimentary archives in which microscopic charcoal is studied (microcharcoal, ca. 10–200 μm in length; Conedera et al., 2009), provide long and continuous records of fire variability (e.g. Beaufort et al., 2003; Daniau et al., 2007; Mensing et al., 1999; Thevenon et al., 2004).

Marine microcharcoal records can be used to validate models under warmer climates than today. However, they only provide a record of the relative changes of biomass burning. Currently, the data-model comparison is limited by the lack of common physical units between data and model output. Relative changes in biomass burning are not directly comparable to model-simulated carbon emissions or burnt areas, or to other components of fire regime such as fire intensity, frequency, severity, and seasonality (Krebs et al., 2010). Microcharcoal quantities preserved in marine sediments must be calibrated against modern fire data in order to provide robust fire metrics and to benchmark quantitative models (Hantson et al., 2016; Hawthorne et al., 2018). Fire regime characteristics are related to weather and climate, the likelihood of plant flammability and human modification (Archibald et al., 2018). Climate and weather conditions determine the type and amount of vegetation and its fuel moisture status, i.e. the drought state of the vegetation, which is why fire occurrence is higher during the summer months, notably in the Mediterranean basin (Trabaud, 1983).

Previous charcoal calibration studies have been conducted in lake sediments to reconstruct fire regime in different biomes (grassland, savanna, temperate forest and Mediterranean forest). Charcoal with a length >100 μm (Adolf et al., 2018), >150 μm (Duffin et al., 2008) and between 125 and 250 μm (Leys et al., 2015) are defined as macrocharcoal by these authors. These studies showed that macrocharcoal accumulation reflects the area of vegetation that burned locally (local burnt area) (Duffin et al., 2008; Leys et al., 2015) or regionally (Adolf et al., 2018), the number of fires and the fire intensity (Adolf et al., 2018). Studies of microcharcoal (between 10 and 500 μm, Adolf et al. (2018); between 10 and 150 μm, Duffin et al. (2008)) showed that microcharcoal accumulation reflects the number of fires (Adolf et al., 2018), the intensity (Adolf et al., 2018; Duffin et al., 2008) and the burnt area (Duffin et al., 2008). Charcoal accumulation in lakes is also controlled by the vegetation surface cover, its biome type and by the fuel amount (Adolf et al., 2018; Marlon et al., 2006). The controlling factors of charcoal accumulation in marine sedimentary records have not yet been investigated.

Here, we present the first study exploring the modern relationships between microcharcoal concentrations in marine sediments and changes in fire regimes on the adjacent landmasses. Microcharcoal influx (or charcoal accumulation rate), i.e. the number of fragments per unit area per unit time, is widely used for biomass burning reconstructions in lake sediments (Marlon et al., 2016). However, we prefer to use microcharcoal concentration in marine sedimentary sequences because the calculation of microcharcoal influx can be hazardous for different reasons, including: 1) coarse age-depth models which lead to imprecise estimates of the sediment accumulation rates, 2) an artificially biased microcharcoal influx due to sediment stretching during the coring or due to high sedimentation rate events, such as Ice Rafted Debris (IRD) deposits (Daniau et al., 2019).

We focused our study on Iberia, one of the most fire-prone regions in Europe (San-miguel-ayanz et al., 2018; Trabaud, 1983). It is also a key area to explore biome and climate influences on charcoal concentrations, as the western Iberian Peninsula is characterised by a north-south climatic gradient, from temperate and wet in the north, with the dominance of the Atlantic forest biome, to hot and dry in the South, dominated by sclerophyllous evergreen Mediterranean vegetation (Polunin and Walters, 1985). In addition, the Iberian margin has provided long marine microcharcoal and pollen records covering the last climatic cycle, over approx. The past 140,000 years, that show higher biomass burning during the Eemian and the Holocene forested interglacials compared to the last glacial period (Daniau et al., 2007). Within the last glacial period, peaks in microcharcoal concentration have been interpreted as an increase in fire frequency and intensity resulting from a change in fuel amount through the development of open Mediterranean forest and heathland (Ericaceae) in response to the Dansgaard-Oeschger (D-O) warming events (Daniau et al., 2007). However, the interpretation of increases in microcharcoal concentration in terms of fire regime characteristics remains an open question.

Microcharcoal concentrations and morphologies here were quantified in marine core-top sediments to document the spatial distribution of microcharcoal concentrations and the type of burnt vegetation. It is generally assumed that the core-top sediments represent late Holocene time spans covering a few hundred to, at maximum, a few thousand years (Müller et al., 1998). However, prior studies have successfully used spatial calibration of marine surface sediment-based proxies to reconstruct different physical and biological ocean and ice properties, such as glycerol dialkyl glycerol tetraether (GDGT) lipids for temperature (Kim et al., 2008; Tierney and Tingley, 2015), dinocyst assemblages for primary productivity and sea ice cover extent (De Vernal et al., 2001; Radi and de Vernal, 2008), foraminifera assemblages (Kucera et al., 2005) and the Long Chain Diol Index (de Bar et al., 2020) for sea surface temperature. Microcharcoal concentrations and morphologies were compared to land and ocean physical-site characteristics, i.e. watershed size, river discharge, suspended sediment load, water depth, marine geomorphology and ocean currents, to evaluate the influence of the collection, transport and deposition of microcharcoal from the production source area to the ocean floor (Fig. 1). The spatial distribution of microcharcoal concentrations was also compared to present-day environmental parameters on land (climate and vegetation) and fire regime characteristics (number of fires, burnt areas, fire radiative power, fire size, fire return interval, fire frequency), to establish a relationship between microcharcoal production and fire parameters (Fig. 1). To support our comparison of the different datasets, we analysed five interface cores covering the past 100 years to test that mean environmental conditions on

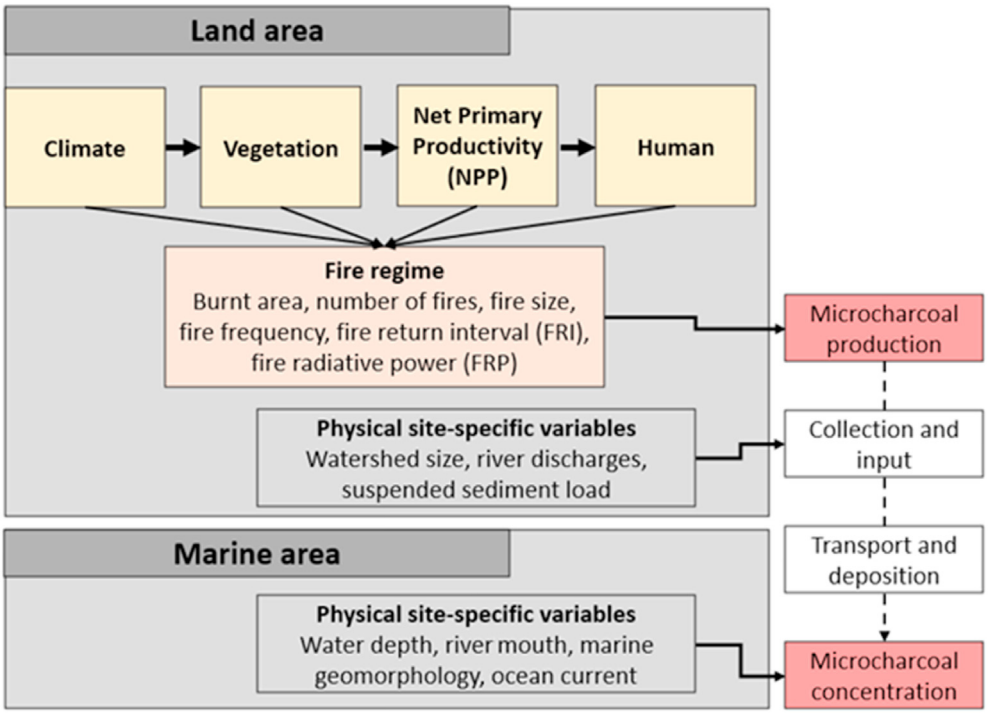

Fig. 1. Variables potentially affecting microcharcoal production on land; the collection, input, transport and deposition of charcoal in the ocean. On land, climate, vegetation, NPP control fire regimes and the production of microcharcoal. Human activities may also affect fire regimes. Physical site-specific variables on land (watershed size, river discharge, suspended sediment load) may impact the charcoal collection and input to the ocean. Physical site-specific variables in the ocean (water depth, distance from the river mouth, marine geomorphology and ocean currents) may impact the transport and deposition of charcoal in the ocean and finally the microcharcoal concentration.

land and in the ocean over the past century do not radically depart from conditions recorded by the instrumental period. Finally, we interpreted the Holocene microcharcoal record from core MD95-2042 (Daniau et al., 2007) in the light of our calibration results.

2. Environmental setting

2.1. Study area and present-day climate, vegetation and fire

The study area encompasses the western Iberian Peninsula and its margin (Fig. 2a) which extends from 37°N to 43°N and includes five major rivers which flow into the Iberian margin (the Minho, Douro, Mondego, Tagus and Sado) and two major rivers which flow into the Gulf of Cádiz (the Guadiana and the Guadalquivir). Other smaller watersheds are drained by the Tambre, Ulla, Lima, Càvado, Ave, Vouga and Mira rivers (Fig. 2b, Table 1). The area is mostly affected by a Mediterranean climate except for the northwestern region which is characterised by an Atlantic climate (Fig. 2a). The region characterised by Atlantic vegetation (Fig. 2a; including here the subatlantic floristic elements defined by Blanco-Castro et al., 1997) is dominated by deciduous oak forests (*Quercus robur, Q. pyrenaica and Q. petraea)*, heath communities (*Erica* and *Calluna*) and *Ulex* whereas, in the Mediterranean vegetation evergreen sclerophyllous forests dominate (Alcara Ariza, 1992; Blanco-Castro et al., 1997).

Specifically, *Q. robur* and *Q. pyrenaica* are dominant trees in the watersheds of the Minho, Tambre and Ulla (Vázquez et al., 2002). The Douro watershed is dominated by *Q. rotundifolia, Q. pyrenaica and Q. faginea* in its eastern part and by *Pinus pinaster* and eucalypts in its western part (Crous-Duran et al., 2014). The western part of the Tagus and the Sado watersheds are colonised by cork forests (*Q. suber)* and holm oaks (*Q. ilex*) (Crous-Duran et al., 2014). The Tagus is dominated by *Q. rotundifolia, Q. pyrenaica,* with *Phillyrea angustifolia* and *Pistacia terebinthus* in its central part and by *Q. rotundifolia* and *Q. faginea* woodlands associated with *Juniperus communis* and *Pinus halepensis* in its eastern part (Vázquez et al., 2002). Thermophilous elements such as *Pistacia lentiscus* and *Olea sylvestris* form the forests in the low altitudes and warmest zones. Deciduous oak forests (*Q. pyrenaica* and *Q. faginea*) associated with *Taxus baccata* dominate the middle altitudes (700–1000 m above sea level). Two types of brush communities are produced by the degradation of this forest, rockrose shrublands (Cistaceae) in zones with precipitation between 600 and 1000 mm and heathlands (Ericaceae) in wetter zones (Morales-Molino et al., 2020). The Guadiana and Guadalquivir watersheds are dominated by *Q. rotundifolia*. In the centre of the Guadiana basin, *Q. rotundifolia* and *Q. pyrenaica* forests are present. In addition, agricultural areas cover almost 50 % of total area of the Iberian Peninsula (Fernández-Nogueira and Corbelle-Rico, 2018) including pasturelands, cereals, vineyards, and olive crops (Grolier online Atlas 2021).

Although the majority of fires in the Iberian Peninsula are human-induced, many fire ignitions from the north of Portugal are triggered by lightning occurring between June and August when the air and climate conditions favour thunderstorms (Pugnet et al., 2010; Vazquez and Moreno, 1998). Different fire regimes are observed in the western Iberian Peninsula with higher fire occurrence in the northwestern region than in the southwestern region (Fig. 2b) (Laurent et al., 2018). A high frequency of small fires occurs in the deciduous forests of the Atlantic bioclimatic region (Vázquez et al., 2002) with a double peak of fires during early spring and summer (Rodrigues et al., 2020). In this region, fires spread in highly flammable and fuelled forests composed of eucalypts (*Eucalyptus globulus*) and several pine species (e.g. *Pinus pinaster* in Portugal and *Pinus radiata* in Spain) (Gonçalves and Sousa, 2017; Silva et al., 2019). The Mediterranean bioclimatic region dominated by sclerophyllous oak forests is affected by intermediate fire

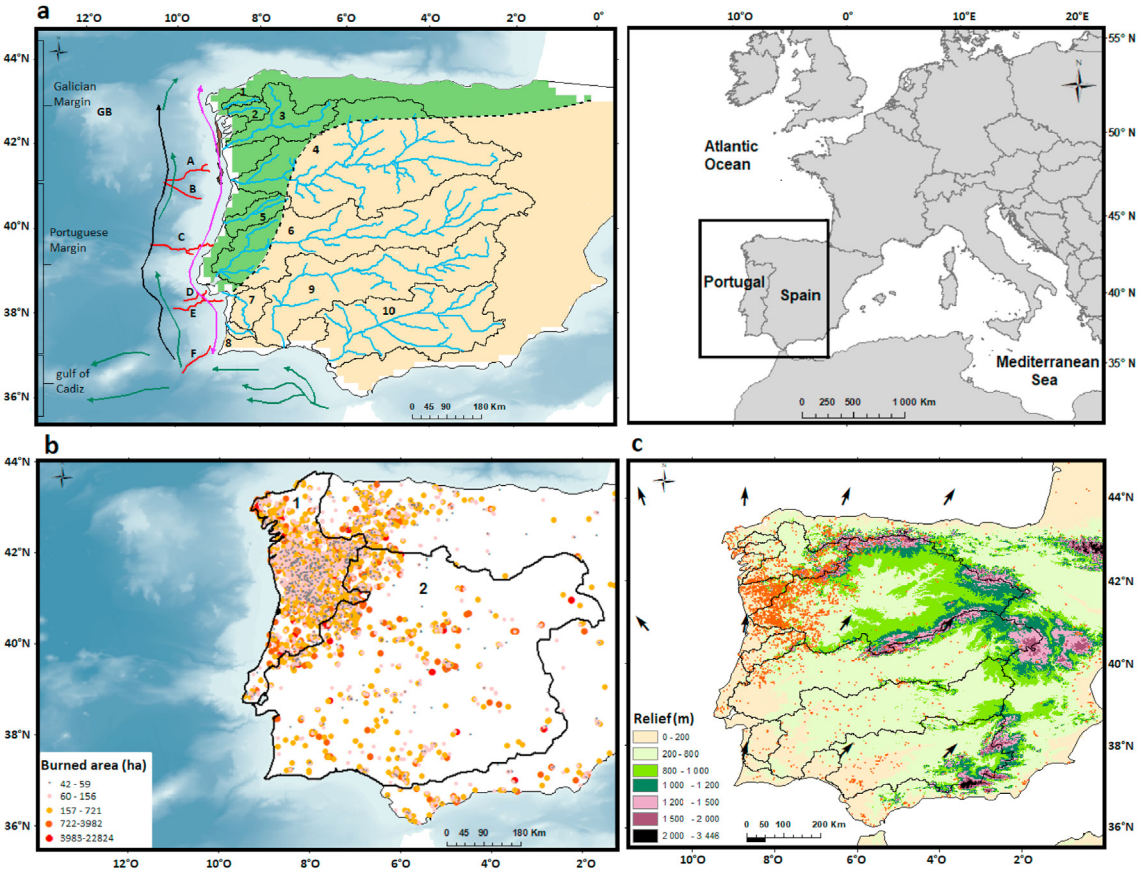

Fig. 2. Study area and environmental context of the Iberian Peninsula. a) The Atlantic (green area) and the Mediterranean (yellow area) vegetation according to Blanco-Castro et al. (1997). The Atlantic vegetation includes here the subatlantic floristic elements defined by Blanco-Castro et al. (1997), rivers (blue lines) and associated hydrographic watersheds (black lines; 1: Tambre, 2: Ulla, 3: Minho, 4: Douro, 5: Mondego, 6: Tagus, 7: Sado, 8: Mira, 9: Guadiana, 10: Guadalquivir). The Galician margin is located between 44°N and 42°N and comprises the Galicia Bank (GB). The Portuguese margin extends between 42°N and 37°N and is cut by six canyons (red lines; A: Porto, B: Aveiro, C: Nazaré, D: Cascais, E: Setubal, F: Sao-Vicente). The Gulf of Cádiz is located between 37°N and 36°N. Ocean currents: the Mediterranean Outflow Water (MOW; green arrows); the Iberian coastal current (ICC; black arrow); the Iberian poleward current (IPC, purple arrow). b) Burnt area (in ha) in the Iberian Peninsula from Laurent et al. (2018): dots represent location of fires between 2001 and 2016; the size of dots represents the size of the burnt areas. Black line outlines the north west (1) and south west (2) pyroregions according to Rodrigues et al. (2020). c) winds at 850 hPa over the Iberian Peninsula from NCEP/NCAR reanalysis between 2001 and 2016 (Kalnay et al., 1996) compared with the topography and the location of fires (orange dots) (Laurent et al., 2018).

Table 1
River and watershed characteristics of the Iberian Peninsula. (1) Oliveira (2002); (2) Mil-Homens et al. (2014); (3) Couso-Pérez et al. (2018); (4) Jouanneau et al. (1998); (5) Van der Weijden and Pacheco (2006); (6) Almeida (2003); (7) Droogers and Immerzeel (2008); (8) Ferreira et al. (2004); (9) Fernández-Delgado et al. (2007); (10) Marta et al. (2001); (11) Portela (2008); (12) Vale and Sundby (1987); (13) Vale et al. (1993); (14) Garel et al. (2009); (15) Guerreiro et al. (2017).

	Length (km)	Hydrographic watershed (10^3 km^2)	River discharge (hm^3 per year)	Suspended sediment load (10^6 t years^{-1})
Major rivers				
Minho	300 (1)	17.081(1) (2)	9.460 (2) 10.375 (1)	N/A
Douro	927(1)	97.682(1) (2)	14.191(2) 14.800 (15)	0.16 (11)
Mondego	227(8)	6.644 (2)	2.492(2)	N/A
Tagus	1000 (4)	80.629 (2)	9.460(2) 9.629 (15)	0.40 (12)
Sado	175 (4)	7.640 (2)	1.261(2)	0.015 (13)
Guadiana	810(10)	66.960 (2)	2.522(2) 2.680 (15)	0.5–1.51 (14)
Guadalquivir	657 (7)	58.000 (7)	0.132–4.224(9)	N/A
Minor rivers				
Tambre	125(3)	1.530 (3)	N/A	N/A
Ulla	132(3)	2.803(3)	N/A	N/A
Lima	180(1)	2.480 (1) (2)	1.955(2)	N/A
Cávado	129(1)	1.589(1) (2)	1.892(2)	N/A
Ave	94(1)	1.390(1) (2)	1.261(2)	N/A
Vouga	141 (5)	3.362(5)	N/A	N/A
Mira	145 (6)	1.576(6)	0.063(2)	N/A

frequency and fire return interval (time between two fires), and medium to large fire sizes (Vázquez et al., 2002) during summer (Rodrigues et al., 2020). Fire frequency is low with a long return interval in the semi-arid, shrubby vegetation.

Fire activity in the Iberian Peninsula is mostly controlled by the length and intensity of the dry season (Turco et al., 2017) with influences of heat wave occurrences (Cardil et al., 2014). In addition it follows an aridity/productivity gradient (Carmona-Moreno et al., 2005; Pausas and Paula, 2012; Vázquez et al., 2002). Fires are more frequent and extensive in wet productive areas with abundant vegetation cover than in dry fuel-limited areas. Seasonal distribution of precipitation is then important. For example, in the deciduous forest of the Atlantic bioclimatic region, spring rains favour fuel accumulation, and very intense summer dry spells favour fuel flammability (Rodrigues et al., 2020; Trigo et al., 2016).

2.2. Geomorphology of the iberian margin and the Gulf of Cádiz and their terrestrial sediment sources

In the adjacent marine environment, the Iberian margin that extends from 43°N to 37°N and from 13°W to 9°W is divided into three geomorphological units (Maestro et al., 2013) (Fig. 2a). The Galicia continental margin (Fig. 2a) extends from 44°N to 41.5°N with a length of 350 km between the coast and the abyssal plain (Vázquez et al., 2008). Its continental shelf extends to about 70 km off the coast with a water depth that varies between 30 m near the coast and 160–180 m delimiting the shelf break (Dias Jouanneau et al., 2002). Further offshore, located about 120 km off the coastline, a seamount, the Galicia bank, rises up to 700 m below sea level (bsl) (Dias Jouanneau et al., 2002; Maestro et al., 2013).

The Portuguese continental margin (Fig. 2a) extends from 41.5°N to 37°N (Maestro et al., 2013). Its continental shelf width varies between 20 and 50 km (Guerreiro et al., 2015) with a slope of less than one degree up to the shelf break located at about 160–200 m bsl. The continental shelf and slope of the Portuguese margin are cut from the north to the south by the Porto, Aveiro, Nazaré, Cascais, Setubal and Sao Vicente (Saint Vincent) submarine canyons (Fig. 2a). The Setubal canyon, with its two branches, is the only one that is connected with modern rivers, the Tagus and Sado rivers (Alves, 2003; Guerreiro et al., 2007; Lastras et al., 2009; Lebreiro et al., 1997).

The Gulf of Cádiz extends from 6°W to 9°W between the Strait of Gibraltar and the Sao Vicente Cape. The continental shelf is 30–40 km wide with the shelf break at 120 m bsl (Lobo et al., 2001). The continental slope is divided into three parts depending on the water depths (Mougenot and Vanney, 1982), between 130 and 400 m, 400–1200 m and 1200–2000 m. Then the rise extends from 2000 m to 4000 m and the abyssal plain from 4000 m.

The Iberian margin receives sediment inputs mainly from the Douro and Tagus rivers but also from the Minho, Mondego and Sado (Dias Jouanneau et al., 2002; Dias, 1987; Jouanneau et al, 1998, 2002; Oliveira, 2002). Sediments can also be transferred seaward by other minor rivers such as the Tambre, Ulla, Lima, Cavado, Ave, Vouga and Mira (Table 1). The Gulf of Cádiz is situated at the mouths of the major Guadiana and Guadalquivir rivers. Rivers supply a large amount of sediments to the Iberian margin and the Gulf of Cádiz (Table 1), although this amount has probably been reduced by the construction of several dams since 1900 (Lehner et al., 2011) which diminish the delivery of sediment by rivers (Kondolf et al., 2014). It is worth noting, however, that some catastrophic floods released large amounts of sediment, such as the one that occurred in 1979 in the Tagus river, an event during which several years of normal river sediment discharge reached the estuary within a couple of days (Vale and Sundby, 1987).

2.3. Oceanic conditions and processes in the transport of fine sediment

On the Iberian margin, the transport of the suspended particulate matter is controlled by the seasonal hydrodynamic context. From September/October to April/May (winter season), enhanced onshore and slightly northward winds on the Iberian margin trigger downwelling currents, while northerly and northwesterly winds trigger upwelling currents the rest of the year (Dias Jouanneau et al., 2002; van Weering et al., 2002; Villacieros-Robineau et al., 2019). The suspended particulate matter released by rivers is transported to the outer shelf in nepheloid layers detaching from the continental slope (van Weering et al., 2002; Oliveira et al., 1999; Villacieros-Robineau et al., 2019) and then northward during downwelling conditions and temporally trapped in the inner shelf during the upwelling season.

Downwelling currents favour the seaward export of sediments on the inner shelf (Oliveira, 2002; Villacieros-Robineau et al., 2019) called the high resuspension inner shelf area (HIRSA) (Fig. S1). The Inshore Coastal Current (ICC) (inner shelf) (Villacieros-Robineau et al., 2019) and the Iberian Poleward Current (IPC) in the upper 200 m of water depth (Frouin et al., 1990) flow northward leading to the northward transport of suspended material (Villacieros-Robineau et al., 2019) (Fig. 2b). On the Galician margin (Fig. 2a) particles are remobilized in the well-developed bottom nepheloid layer (BNL) (Oliveira et al., 1999; Villacieros-Robineau et al., 2019).

During the upwelling season, the weak energy and well developed surface nepheloid layers permit pelagic vertical sinking (Villacieros-Robineau et al., 2019) and fine sediments are temporally trapped in the Minho, Douro and Tagus mud patches located on the continental shelf in front of the river mouths (Dias Jouanneau et al., 2002; Jouanneau et al., 1998). During this season the ICC flows southward on the inner shelf but the BNL is sufficiently developed offshore, allowing sediments to be exported westward and picked up by the IPC (Villacieros-Robineau et al., 2019). In addition, modelling work conducted by Otero et al. (2013) reported an episode of upwelling favourable winds during the winter season. During this episode, particles were exported southwestward off the Douro and Minho rivers. Particles released at the mouth of the Minho (42°N) did not reach the latitude of the Douro river mouth (41.5°N) and particles released at the mouth of the Douro did not reach the mouth of the Mondego (40.2°N), even when the ICC flowed southward during upwelling conditions.

The canyons incising the Iberian margin act as preferential conduits for transporting sediments from the continental shelf to the deep sea all year long (Fig. 2a). However, the particle remobilisation in canyon heads during the downwelling season amplifies the amount of supplied material (Jouanneau et al., 1998; Lastras et al., 2009; Villacieros-Robineau et al., 2019). The Nazaré canyon acts as a major conduit for the transport of particulate matter to the deep sea as it crosses the continental shelf (Schmidt et al., 2001), depriving the rest of the shelf of sediments down to Lisbon.

Beyond the continental shelf, on the continental slope and at the bottom of the slope, the Eastern Atlantic Central Water (ENACW) flows northward between 100/200 m and 500 m of water depths (Hernández-Molina et al., 2011) (Fig. S1). The intermediate circulation is dominated by the Mediterranean Outflow Water (MOW), which flows northward along the Iberian coast at depths between approx. 500 m and 1500 m (Maestro et al., 2013). The deep circulation is dominated by the North Atlantic Deep Water (NADW) that flows southward beneath 1500 m bsl (Hernández-Molina et al., 2011). In the Gulf of Cádiz the North Atlantic Superficial Water (NASW) and the North Atlantic Central Water (NACW) constitute the superficial oceanic circulation that flows to the southeast on the continental shelf and the upper part of the continental slope, at

respective water depths of 0–300 m for the former and 300–600 m for the latter (Hernández-Molina et al., 2011). Below this, the Mediterranean Outflow Water (MOW) splits into two branches which flow to the west at depths between 400 and 600 m and between 600 and 1400 m. The NADW follows an anti-cyclonic gyre circulation in the Gulf (Hernández-Molina et al., 2011).

3. Material and methods

3.1. Marine surface sediments

The sample dataset includes 100 core-top sediment samples from the ocean floor and two samples collected at the mouths of the Promira and Sado rivers. The 100 samples were collected from several marine sedimentary cores from 13 oceanographic cruises carried out between 1981 and 2013 on the Iberian margin (8°W-13°W/43°N-36°N) (Fig. 3), recovered by various coring methods (mostly box, piston and multicore) (Table S1). Samples were recovered in the most superficial sections of the sedimentary cores, depending upon the availability of sediment. Our dataset contains 23 samples taken at core depths 0–0.5 cm, 50 samples at 0–1 cm, 22 samples at 0–2 cm, 4 samples at 2–2.5 cm and 1 sample at 4–5 cm core depths. 33 samples were collected from cores retrieved in the Galician continental margin, including 21 samples located between 9°W and 13°W and 43°N and 42°N and distributed between the continental slope and the abyssal plain (1129 m and 5378 m bsl). The 12 remaining samples were located off the Douro river between 8°W and 10°W, and on the continental shelf and slope (51 m and 1989 m bsl) between the Porto and Aveiro canyons. 60 samples were collected from cores retrieved in the Portuguese margin including 12 off the Mondego river, north of the Nazaré canyon, between 8°W and 10°W. Their location is limited to the continental shelf and slope (28 m and 1808 m bsl). The 48 remaining samples are located between 8°W and 11°W between the Nazaré and Sao-Vicente canyons on the continental shelf and slope (13 m and 3731 m bsl). A value of 0 m depth was arbitrarily assigned to the two samples collected at the mouths of the Sado and Mira rivers. We explored the temporal variability in microcharcoal concentrations using five interface cores located in the Galician margin (Fig. 3), the PE109-97-Station4 (10 samples, sampled every 0.5 cm, covering the period 1897–1969), the PE109-97-Station8 (6 samples, every 0.5 cm, 1888–1948), the PE109-97-Station9 (6 samples, every 0.5 cm, 1886–1948), the PE109-97-Station6 (8 samples, every 0.5 cm, 1898–1964) and the Pech7I (8 samples, every 0.5 or 1 cm, 1935–2005).

Our compilation of dating information, when available or obtained by $^{210}Pb_{xs}$ measurements on the bulk sediment, show that the samples cover from one decade to a few centuries of environmental changes (Table S1; Table S3). Among the 102 samples, two are modern, nine are dated less than 20 years, two less than 60 years, four less than 100 years, one less than 350 years and two samples less than 500 years. 12 samples are estimated to be of the late Holocene age and 10 of the Holocene age. No information regarding dates is available for the remaining 60 samples.

3.2. Microcharcoal concentrates and their quantification by image analysis

The chemical treatment applied to obtain microcharcoal concentrates follows that of Daniau et al. (2007). About 0.2 g of dry bulk sediment was treated with 5 ml of 37 % hydrochloric acid (HCl), to eliminate the calcium carbonates, and 5 ml of 37 % nitric acid (HNO_3) in a water bath at 70 °C for an hour, followed by the addition of 10 ml of 33 % hydrogen peroxide (H_2O_2) to digest the organic matter. Hydrogen peroxide does not bleach charcoal (Herring, 1985; Rhodes, 1998). The samples were transferred to test tubes and centrifuged at 3000 rpm for 7 min with distilled water to clean and remove the supernatant before using 25 ml of 70 % hydrofluoric acid (HF) to eliminate the siliceous material, followed by rinsing with HCl to remove colloidal SiO_2 and silicofluorides formed

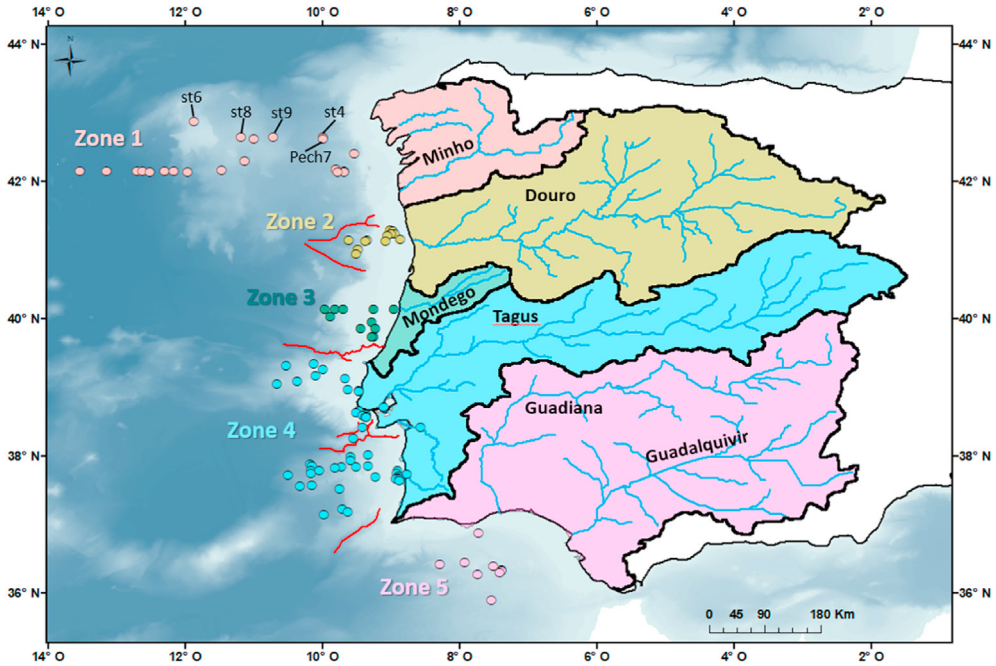

Fig. 3. Location of samples (colour dots) and definition of microcharcoal preferential source areas (coloured areas on land) drained by major rivers. Zone 1 drained by the Tambre, Ulla and Minho rivers; Zone 2 by the Douro; Zone 3 by the Mondego; Zone 4 by the Tagus and Sado; Zone 5 by the Guadiana and the Guadalquivir. Red lines underline the location of the submarine canyons. Interface cores are indicated (Pech7I and the 4 stations of PE109-97). (For interpretation of the references to colour in this figure legend, the reader is referred to the Web version of this article.)

during the HF digestion and then distilled water for cleaning the residue. A dilution of 0.1 (distilled water) was applied to the residue and the suspension was then filtered on a membrane of 0.45 μm porosity and 47 mm in diameter. A portion of this membrane was mounted onto a PMMA (Poly Methyl Methacrylate) slide with ethyl acetate. The slides were hand polished with a PRESI polisher (The CUBE) on a very soft flock cloth for 4 min using alumina solution of 400 Angström. The slides were scanned with an automated Leica DM6000M microscope at × 500 magnification in a controlled transmitted light adjustment to detect and measure microcharcoal (length >10 μm) as being black, opaque, and angular (Boulter, 1994), using a threshold value in tint, saturation and lightness (TSL) colour space. Petrographic criteria in reflected light were used to secure the identification of microcharcoal in transmitted light. For each sample the microcharcoal concentration was calculated by number of particles per gram dry weight (CCnb in nb/g) as well as by total area of all microcharcoal in one sample per gram dry weight (CCsurf in mm^2/g). This is to avoid the overrepresentation of CCnb as the result of potential fragmentation during production or transport. The shape was also analysed using the elongation, i.e. the particles' length to width ratios.

3.3. Microcharcoal preferential source areas

Particulates of microcharcoal are mainly transported by water and winds (Millspaugh and Whitlock, 1995; Patterson et al., 1987) before being integrated into the sediments either in lakes or in the marine realm. The specific gravity of dry microcharcoal particles is 0.3–0.6 (Turner et al., 2004) with a length between 10 and 100 μm (Whitlock and Larsen, 2002). Water saturated microcharcoal particles have a specific gravity of 2.2, similar to that of pollen grains (Turner et al., 2004). Thus, microcharcoal transport and sedimentation in the ocean is likely to be similar to that of pollen grains. Pollen studies of deep-sea surface sediments close to river mouths showed that fluvial transport is the dominant delivering process of pollen grains to offshore areas as it is the case in the western Iberian margin (Naughton et al., 2007) while airborne pollen transport prevails in marine sediments located further than 300 km offshore, weakly influenced by rivers (e.g.). Biological and chemical processes in the upper part of the water column, such as agglomeration of dust and other microparticles into faecal pellets and marine snow, increase significantly the settling rates of pollen grains so that they cross the water column with a relatively high speed (estimated at about100 m/day in the Atlantic water column, Hooghiemstra et al. (1992)) before being deposited on the sea floor in the absence of strong lateral and bottom currents (Mudie and McCarthy, 2006; Turon, 1984).

The latitudinal pollen distribution in marine surface sediments represents the vegetation distribution in the adjacent continent (Dupont and Wyputta, 2003; Heusser and Balsam, 1977; Hooghiemstra et al., 2006; Mudie, 1982). In particular, pollen assemblages from surface marine sediments collected along the Iberian margin clearly distinguish the vegetation formations of the adjacent hydrographic basins of the western Iberian Peninsula (Morales-Molino et al., 2020; Naughton et al., 2007). Thus, microcharcoal preserved in marine core-top sediments is assumed to reflect an integrated image of the recent regional fire regime of the adjacent continent.

Wildfire plumes may raise high into the atmosphere depending on the fire radiative power (Sofiev et al., 2013) and may lift and transport charcoal particles to different distances from the fire. Clark (1988) showed that aeolian charcoal particles of a small length can be transported further away than larger particles. Microscopic charcoal particles (about 5–200 μm in length) are deposited a few hundred metres away from the fire, up to a few dozen kilometres for a column injection of about 1 km height. The maximum injection height above the Iberian Peninsula is about 1500–2000 m (Sofiev et al., 2013). Our microcharcoal particles with a length between 10 and 125 μm could, therefore, be deposited a few hundred metres away by surface wind from the fire location, up to a few dozen kilometres by high altitude winds. Vachula, 2021 suggests that a source area of 50 km should be considered for all size fractions. Anti-cyclonic circulation patterns associated with warm and dry winds from inland leading to very high values of burnt area occurred during August (Trigo et al., 2016). Dominant winds at 850 hPa (1450 m) blow northward along the coast and northeastward over the centre of the Iberian Peninsula (Fig. 2c). Given the direction of the winds along the coast, some charcoal may potentially travel from each basin to the nearest one to the north (from the Sado to the Tagus, the Tagus to the Mondego, the Mondego to the Douro and, the Douro to the Minho). Inland, charcoal may be transported from the Guadalquivir to the Guadiana and, from the Guadiana to the Tagus hydrographic basin.

The Guadalquivir, Guadiana, Tagus, Sado and the eastern part of the Douro hydrographic basins are located in the pyroregion with sparse fires and low values of burnt area (Trigo et al., 2016). A few number of fires are located along the northern borders of those basins, suggesting that a limited transfer of charcoal may occur, 50 km from the fire source (Vachula et al., 2021). Also, given the relief, it is unlikely that a substantial amount of charcoal would be transported from the Tagus to the Douro. We cannot exclude some contributions from the Tagus to the Mondego, from the Mondego to the Douro and from the Douro to the Minho.

Based on the studies above and on the sediment input and transport of fine particles to the Iberian margin (sections 2.2 and 2.3), we grouped our marine microcharcoal samples in five zones depending on their preferential source areas on land (Fig. 3). Zone 1 includes 21 marine samples located between 44°N and 42°N and their preferential sediment source area associated to the Minho, Tambre, Ulla and Lima watersheds. Zone 2 comprises 12 samples located between the Porto and Aveiro canyons, the associated major Douro watershed and Ave, Vouga and Càvado minor watersheds. Zone 3 includes 11 samples located between 38.5°N and 38.2°N and the hydrographic watershed of the Mondego. We acknowledge that zones 1 and 2 may also be affected by sediments released by the Douro and the Mondego, respectively. Zone 4 groups 48 samples between the Nazaré and Sao-Vicente canyons, associated with the major watersheds of the Tagus and the Sado as well as the Mira and other small watersheds. Most of the fine particles in the whole southern half of the Iberian margin come mainly from the Tagus and Sado rivers, whose particles exported offshore propagate both to the north and the south carried out by ocean currents (Dessandier et al., 2016; Jouanneau et al., 1998). The Tagus, Sado, Mira, Guadiana and Guadalquivir basins belong to the same pyro-region (Fig. 2c) in which the fire regime is similar (Rodrigues et al., 2020). However, we separated watersheds from the rivers which flow into the Iberian margin (Tagus, Sado, Mira) from those which flow into the Gulf of Cádiz (Guadiana, Guadalquivir). Zone 5 includes therefore 8 samples located in the Gulf of Cádiz associated with the Guadiana and Guadalquivir main watersheds and other small watersheds located between 5.5°W and 9°W.

3.4. Explanatory variables, data sources, treatments and analyses

Climate data, temperature and precipitation were extracted from the CRU (Climatic Research Unit) database (Version: CRU CL v. 2.0, grid with spatial resolution: 10 min, period: 1961–1990) of New et al. (2002). The Net Primary Productivity (NPP) data come from the GFED4s (Global Fire Emissions Database that includes

Small fires) (Version: GFED4s, grid with spatial resolution: 0.25°, period: 1997–2015 (Giglio et al., 2013)). Fire regime data were derived from the global database of fire patches (FRY_MCD64) from the MODIS sensors on board the Aqua and Terra satellites (Laurent et al., 2018), i.e. the burnt area in hectares (ha) and the Fire Radiative Power FRP (the energy emitted by fire measured in Watts) for each fire over the period 2001–2016 (Laurent et al., 2019). From this database, we calculated the fire return interval (FRI) by dividing the number of days in one year (using 365 days per year) by the number of fires per year for each zone.

The FRY database also contains the four main vegetation types according to the UNLCCS classification (United Nations Land Cover Classification System) called "burnt species" which burn each year. Based on the conversion carried out in the work of Poulter et al. (2015), the four main burnt species were grouped into four groups "Burnt Tree", "Burnt Shrub", "Burnt Grass" and "Burnt Non-vegetated", and into three categories "Burnt Open vegetation" dominated by grasses and shrubs, "Burnt Mixed vegetation" dominated by trees and shrubs, "Burnt Closed vegetation" dominated by trees (Table S2).

Climate, vegetation and fire data were averaged annually or seasonally (boreal winter season from December–February, DJF; spring from March–May, MAM; summer from June–August, JJA; autumn from September–November, SON) according to microcharcoal preferential source areas (section 3.4), using ArcGIS for Desktop software. We performed a principal component analysis (PCA) using the package FactoMineR (Lê et al., 2008) on the seasonal land climate and vegetation data (Temperature, Precipitation, Net Primary Productivity) to explore environmental patterns on land which could affect fire regimes and charcoal production. Initial exploration of climate data indicated that winter and summer temperature and precipitation differences between the north and the south of the Iberian Peninsula are clearly seen when using mean annual temperature (MAT) and mean annual precipitation (MAP) (MAP and MAT are significantly and positively correlated with seasonal values, Fig. S2 and S3). However, differences in the net primary productivity between the north and the south of the Iberian Peninsula are only evident when using winter and summer seasons, and muted using annual average NPP (Fig. S4). Annual climate data and seasonal NPP were then used to explore relationships with microcharcoal concentrations. The distribution pattern of microcharcoal concentrations and elongation ratio values between zones were explored using boxplots. We used the Student's T-test for the averages and the Kruskall-Wallis test for the medians in order to explore the differences and similarities of microcharcoal concentrations and elongation values between zones (Fig. S7).

Cluster analysis (Fig. S9) was carried out on microcharcoal concentrations and water depths of samples (and elongation ratio values and water depths) using the single linkage (nearest neighbour) algorithm and stratigraphically constrained clustering (Past software, Hammer et al., 2000). Clusters are joined based on the smallest distance between the two groups and only adjacent rows, or groups of rows, are joined during the agglomerative clustering procedure. No additional information was obtained when considering the distance to the coast as it is significantly and positively correlated with the water depths of samples (Fig. S10).

4. Results

4.1. Microcharcoal concentrations and elongation

The concentrations of microcharcoal, CCnb (microcharcoal concentration by number of particles per gram) and CCsurf (microcharcoal concentration by total area of all microcharcoal in one sample per gram) (Table S3), are positively correlated ($r = 0.92$, $P < 0.001$) (Fig. S5). Thus, CCnb can be used to describe the spatial distribution of microcharcoal concentrations. The CCnb is heterogeneous on the Iberian margin, with concentrations varying between 0 nb/g (4 samples) and 1.1×10^6 nb/g (Fig. 4a). However, the analysis of microcharcoal concentrations within the previously defined areas shows a marked latitudinal variation in their distribution (Fig. 4b). Zones 3 and 4 present the highest mean concentrations (3.3×10^5 nb/g and 3×10^5 nb/g, respectively), followed by zones 2 (1.8×10^5 nb/g), 5 (8.1×10^4 nb/g) and 1 (5.1×10^4 nb/g). Medians of microcharcoal concentration are overall higher in zones 3 and 4 compared to 1, 2 and 5 (Fig. 4b). The mean values of microcharcoal concentration are similar for zones 4 and 3, and for zones 1, 2 and 5, respectively (Student's T-test for the mean; p-value >0.05) (Fig S7). Medians of zones 3 and 4 are similar to zone 2 and are significantly different from zones 1 and 5 (Kruskal-Wallis test for the median; p-value <0.05).

The sediment density and sedimentation rates are not available to calculate influx for each core-top sample. We further explore whether the spatial distribution of microcharcoal concentration is time dependent for samples with an estimated age (Table S1). Zones 3 and 4 present a higher number of microcharcoal per gram per year compared to zones 1 and 5 (Fig. S6), similar to the spatial distribution of microcharcoal concentration per zones (Fig. 4b). We suggest, therefore, that the spatial distribution of microcharcoal concentrations is not dependent on the sedimentation rate.

Microcharcoal up to 125 μm in length were observed. Mean microcharcoal elongation ratios vary between 1.43 and 2.96 (Fig. 4c). There are no differences between mean elongation values between zones (Fig. S7). However, the medians of zones 4 and 1 are significantly different (Fig. S7). In addition, although the mean elongation values of microcharcoal (Fig. 4c) are similar between zones (Fig. S7), the individual elongation ratio values present a high variability, between 1.07 and 10.33 (Fig. 4d). In particular, zones 3 and 4 present the highest number of very elongated particles (ratios between 3 and 10.33).

Results show that the mean microcharcoal concentration increases with decreasing latitudes off the westernmost Iberian margin, and more elongated microcharcoal particles are observed in zones 3 and 4. In addition, a high variability of microcharcoal concentrations is also observed within each zone (Fig. 4a).

The comparison between microcharcoal concentration in marine samples and the different datasets (climate, fire regime and vegetation data) could be biased as the periods of data do not overlap. However, Shafer et al. (2003) showed that spatial variations of climate were larger than temporal variations over the period 1961–2008. Therefore, this temporal mismatch should not influence the results of our comparison, and the relative differences between hydrographic basins in terms of climate, vegetation and fire regimes are likely to have been preserved over the past decades. The distribution of microcharcoal concentrations according to depth in the interface cores located within zone 1 (Fig. 3) is within the range of the modern spatial variability (Fig. S8). This suggests that mean environmental conditions on land and in the ocean over the past 100 years, corresponding to these past century biomass burning records, did not radically depart from conditions recorded by the instrumental period, therefore supporting our comparison of the different datasets.

4.2. Microcharcoal production in the western Iberian Peninsula and concentrations in marine surface sediments

4.2.1. Climate and net primary productivity (NPP)

The principal component analysis yielded two dimensions with eigenvalues of 44.3% and 25.7%, respectively (Fig. 5), 70% of the

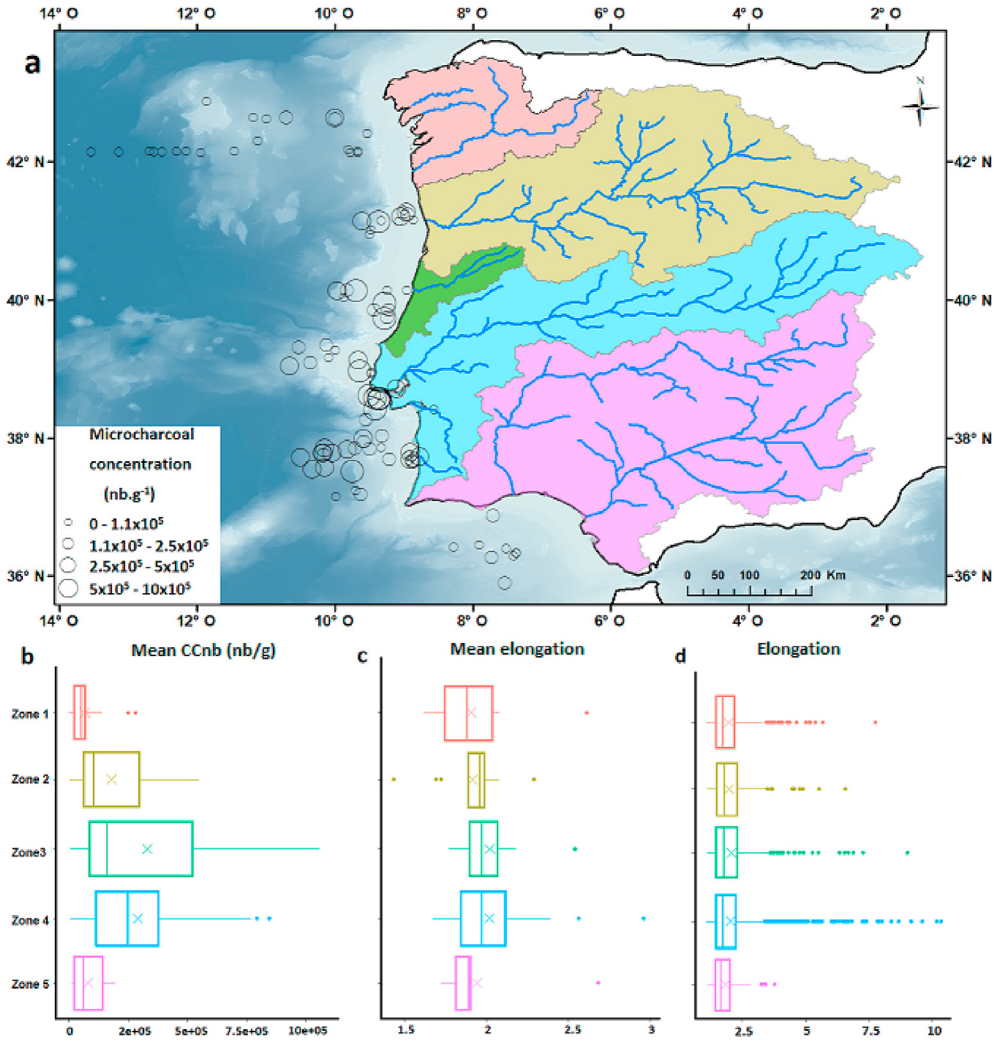

Fig. 4. Spatial distribution of microcharcoal concentrations. a) Microcharcoal concentrations in samples located in the Iberian margin and the Gulf of Cádiz; b) Boxplot of mean microcharcoal concentrations in each zone; c) Boxplot of mean elongation of microcharcoal in each zone; d) Boxplot of individual elongation value of microcharcoal in each zone.

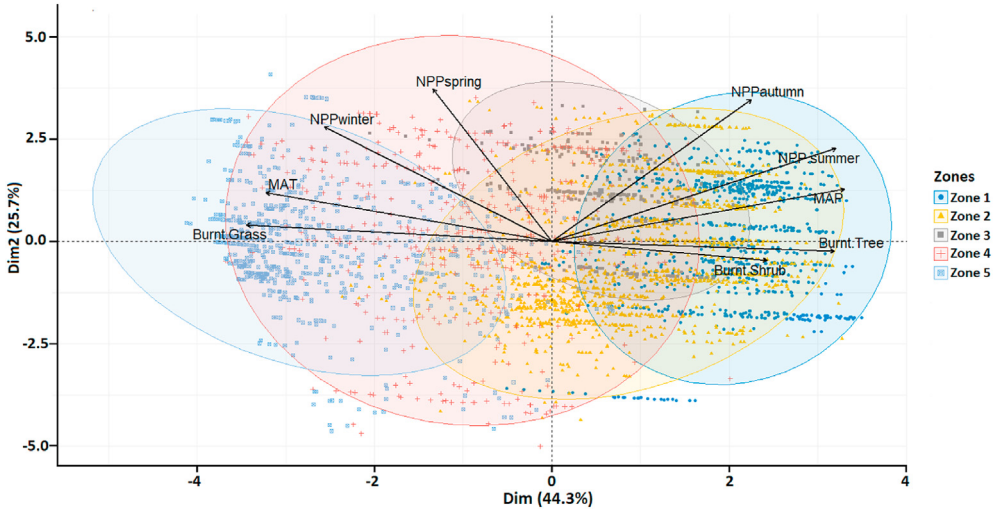

Fig. 5. Results of the PCA of fires and environmental data for each fire between 2001 and 2016 (Laurent et al., 2018). Burnt Grass, Burnt Shrub and Burnt Tree derived from the FRY database (Laurent et al., 2018). Net primary productivity for all seasons: NPP_winter, NPP_spring, NPP_summer, NPP_autumn, Mean Annual Temperature (MAT) and Mean Annual Precipitation (MAP) derived from the GEFD4s database (Giglio et al., 2013). Preferential source areas of microcharcoal: zone 1 (blue circle), zone 2 (yellow circle), zone 3 (grey circle), zone 4 (red circle), zone 5 (blue circle). (For interpretation of the references to colour in this figure legend, the reader is referred to the Web version of this article.)

variation therefore being explained by the first two eigenvalues. Zones 1 and 2 are projected on the positive PC1 axis, characterising a cold and humid climate with a high NPP in the summer and autumn, while zones 4 and 5 are on the negative PC1 axis, characterising a hot and dry climate with a high NPP in the winter and spring. Zone 3 is less well characterised on the PC1 axis but seems more characterised on the PC2 axis with a wet and warm climate and high annual NPP values. The annual NPP spatial variability, which reflects major vegetation type distribution (Running et al., 2000), is high in the northern region dominated by the temperate forest and low in the southern part occupied by sclerophyllous trees and shrubs.

High microcharcoal concentrations in marine zones 3 and 4 are associated with terrestrial zones characterised by a warm and dry climate, with a low annual NPP but a high winter NPP; whereas low microcharcoal concentrations (zones 1 and 2) are characterised by a cool and wet climate, with a high annual and summer NPP. Although terrestrial zone 5 is characterised by a similar climate and NPP conditions as zone 4, its mean microcharcoal concentration is lower.

4.2.2. Fire regimes

Low microcharcoal concentrations in zones 1 and 2 are associated with a high number of fires (812 and 1584 fires in total over the period 2001–2016, respectively) of small size (593 and 614 ha, respectively) and of low intensity (mean FRP: 66 W) with a short fire return interval (7 and 4 days, respectively) (Fig. 6). However, zone 2 presents a high burnt area (9,72 $\times$ 10^5 ha) while zone 1 presents a low burnt area (2,35 $\times$ 10^5 ha). Those fire types occur in cool and wet climate conditions with a high summer NPP (Fig. 5). In zone 5 a low microcharcoal concentration is associated on land with similar fire regimes characteristics, i.e. a moderate burnt area of 6.73 $\times$ 10^5 ha, a high number of fires (927 fires) of small size (726 ha in average) and of low intensity (mean FRP: 40 W) with a short fire return interval (6 days) (Fig. 6), whereas the climate is hot and dry and the NPP is high in winter (Fig. 5). High microcharcoal concentrations in zones 3 and 4 are associated with a lower number of fires (243 and 503, respectively) and larger fires (972 and 1485 ha, respectively) than in zones 1 and 2 (812 and 1584 fires, and 593 and 614 ha, respectively). However, zone 3 presents a very low burnt area (2.35 $\times$ 10^5 ha) while zone 4 presents a high burnt area (7.47 $\times$ 10^5 ha). In addition, fire intensity is higher (mean FRP: 89 W) and the fire return interval lower (24 and 12 days, respectively), in a hot and dry climate, the NPP being important all year round in zone 3 and only during winter in zone 4.

4.2.3. Burnt species

The low mean microcharcoal concentrations and low mean elongation ratios are associated with the burning of species corresponding to closed (42.3 %) and mixed (39.4 %) vegetation (in zone 1 (Fig. 7) and with the burning of open vegetation at 92.6 %, with 76.4% of it corresponding to managed grass in zone 5 (Table S2). The relatively low mean microcharcoal concentrations and high mean elongation ratio in zone 2 are associated with mixed (43.7 %), open (32.8 %) and closed (23.5 %) vegetation. The high mean microcharcoal concentrations and high mean elongation ratios are associated with the burning of open (37 %), mixed (37.5 %) and closed (25.5 %) vegetation in zone 3, and with the burning of open (67.6 %), closed (17.1 %) and mixed (15.3 %) vegetation in zone 4 (Fig. 7).

4.3. Physical site-specific variables on land and in the ocean and relationships with the collection, transport and deposition of microcharcoal

4.3.1. Size of watershed, river discharges and suspended sediment loads

Low mean microcharcoal concentrations are observed off the coast of watersheds of small (Minho) and large (Douro, Guadiana and Guadalquivir) size rivers, of low (Guadiana and Guadalquivir) and high (Douro) river discharges, and of low (Minho) and high (Douro, Guadiana and Guadalquivir) suspended sediment loads (Table 1). High mean microcharcoal concentrations are observed off watersheds of small (Sado and Mondego) and large (Tagus) size rivers, of low (Mondego, Sado) and high (Tagus) river discharges, and of low (Sado, Mondego) and high (Tagus) suspended sediment loads.

4.3.2. Water depth, marine geomorphology and ocean currents

The hierarchical grouping (clustering) considering microcharcoal concentrations and water depth of samples highlights seven groups (Fig. 8a and Fig. S9a). Four groups (group 1 with 10 samples, group 2 with 9 samples, group 3 with 12 samples and group 4 with 10 samples) are located on the shelf between 0 and 506 mbsl (Fig. 8b). Group 5 (40 samples between 598 and - 2280 m bsl) and group 6 (11 samples between 2323 and 3162 m bsl) are located on the upper and bottom of the slope, respectively. Group 7 (10 samples, between 3557 and 5357 m bsl) corresponds to the abyssal plain.

Mean microcharcoal concentration values of groups 1, 2 and 3 are significantly similar, and different from group 5 (Student T-test

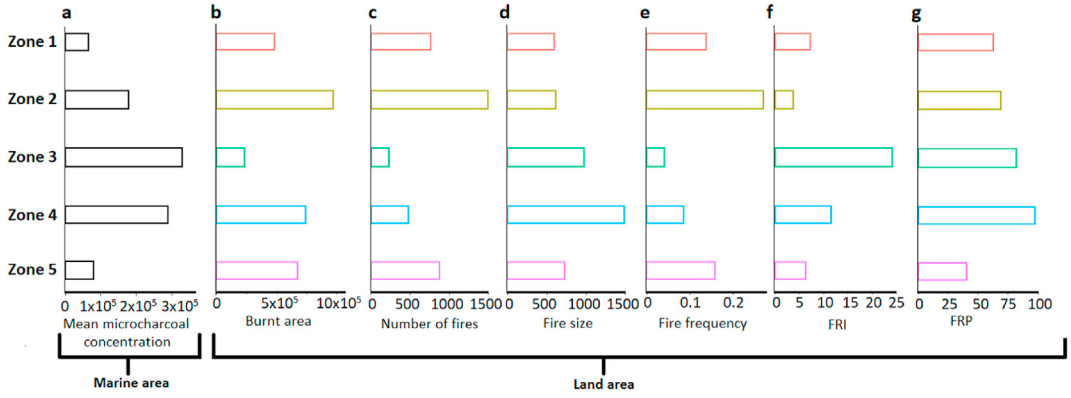

Fig. 6. Microcharcoal concentrations *versus* fire regimes on the Iberian Peninsula over the period 2001–2016 (FRY database) (Laurent et al., 2018), for each zone. a) mean microcharcoal concentration in marine zones (CCnb); b) to g) correspond to total burnt area (in ha), total number of fires, mean fire size (in ha), fire frequency, mean Fire Return Interval (FRI, in days), mean Fire Radiative Power (FRP, in Watts).

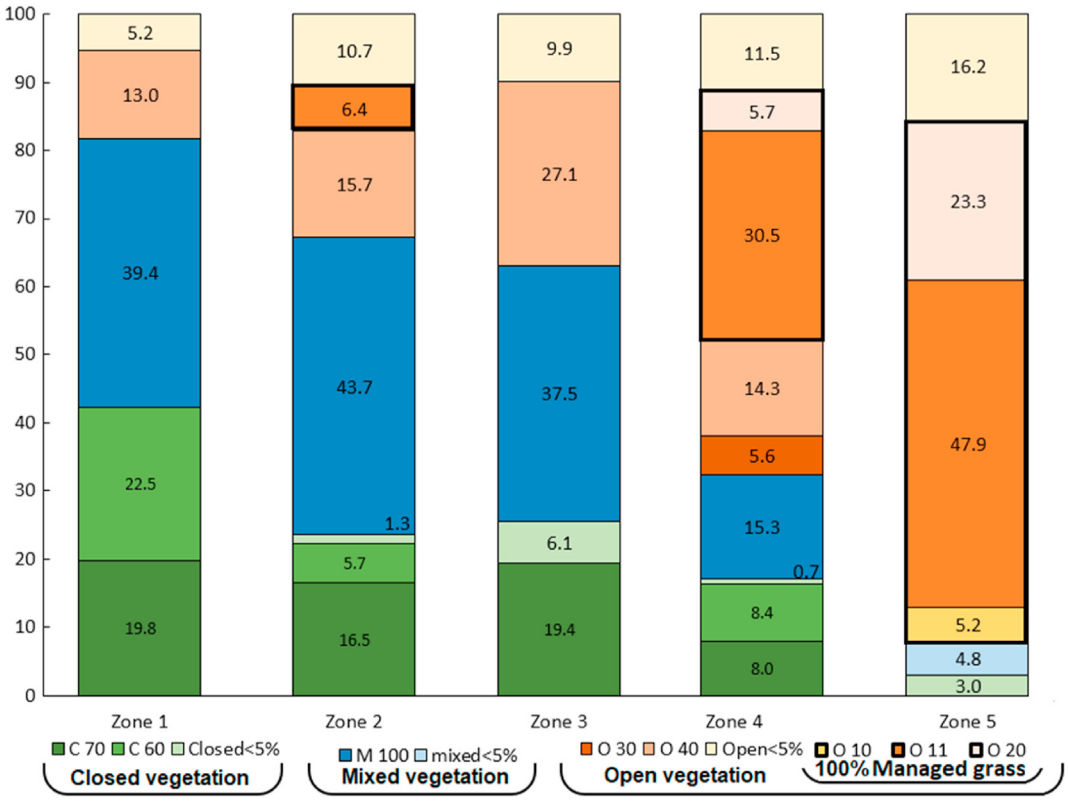

Fig. 7. Burnt species from the FRY database (Laurent et al., 2018) classified following the United Nations Land Cover Classification System (UNILCSS). Green colours correspond to closed vegetation: C60 (tree cover, broadleaf, deciduous, closed to open (>15%)), C70 (tree cover, needleleaf, evergreen, closed to open (>15%)), closed<5 % (sum of burnt species percentages from the closed vegetation present <5 %). Blue colours correspond to the mixed vegetation: M100 (mosaic tree and shrub (>50%)/herbaceous cover (<50%)), mixed<5 % (sum of burnt species percentages from the mixed vegetation present <5 %). Orange colours correspond to the open vegetation: O10 (cropland, rainfed), O11 (herbaceous cover), O20 (cropland, irrigated or post-flooding), O30 (mosaic cropland (>50%) nat. veg. (tree, shrub, herb.) (<50%)), O40 (mosaic nat. veg. (tree, shrub, herb.) (>50%)/cropland (<50%)), open<5 % (sum of burnt species percentages present in the open vegetation <5 %). Numbers in the rectangles correspond to percentages of the different burnt vegetation type. (For interpretation of the references to colour in this figure legend, the reader is referred to the Web version of this article.)

for the mean; p-value >0.05) (Fig. 8a, Fig. S12a). Mean microcharcoal concentrations of groups 5, 6 and 7 are different. Group 4 share common features with other groups. The clustering considering microcharcoal elongation values and water depths of samples highlight six groups with similar means and medians (Figs. S11 and S12).

As a general pattern, the mean microcharcoal concentrations decrease from the shelf (groups 1 to 4) to the upper slope (group 5), increase from the upper slope to the bottom of the slope (group 6) and decrease again from the slope to the abyssal plain (group 7). The increase of mean microcharcoal concentrations along the slope is observed. 20 samples located between the Setubal and the Sao-Vicente canyons on a gentle and regular continental slope are spatially well distributed from the upper to the bottom of the slope at different water depths ranging from 506 to 3731 m bsl (Fig. 8b, black polygon, groups 5 and 6). This zone presents a sufficient number of samples to explore the influence of water depth on microcharcoal concentrations within a specific depositional area. Mean microcharcoal concentrations and water depths (negative values) are negatively correlated ($r = -0.63$, $P < 0.01$, Fig. 8c.

5. Discussion

5.1. Microcharcoal in marine sediments as a tracer of fire regimes

The results presented above suggest that differences between groups of mean microcharcoal concentrations depend on large-scale environmental variations on the adjacent landmasses (at a sub-continental scale) which affect the production of charcoal (Fig. 1). Mean microcharcoal concentrations in the marine realm can be either high or low depending upon the watershed size, the river discharge and the suspended sediment load. The study of Marlon et al. (2006) indicated that charcoal influx in lake sediments increases with watershed size due to a higher burnable area. In contrast, our results suggest that physical site-specific variables on land, i.e. the watershed size, river discharge and suspended sediment load do not impact the capture and transport of microcharcoal within the watershed and microcharcoal input to the ocean. In addition, studies on North Pacific marine sediments showed that the distribution pattern of charcoal concentrations was similar to the distribution pattern of charcoal accumulation, suggesting that the distribution pattern of charcoal concentration is not an artefact produced by varying degrees of sediment dilution (Herring, 1985; Smith et al., 1973).

Our study, in contrast to previous studies of microcharcoal in terrestrial (Duffin et al., 2008; Tinner et al., 1998) and marine areas (Mensing et al., 1999), indicates an opposite relationship between microcharcoal concentration and the number of fires and no relation with the burnt areas. This finding in our marine sediments is consistent with the study of Whitlock and Larsen (2002), which suggests that temporal increases in microcharcoal abundances in lakes reflect a change in fire regime, rather than a strict change in the number of fires or area burned, when fires suddenly affect previously high biomass fire-free areas instead of low biomass fire-prone areas. High values of fire size, FRI and FRP in zones 3 and 4 are associated with high mean microcharcoal concentrations in the

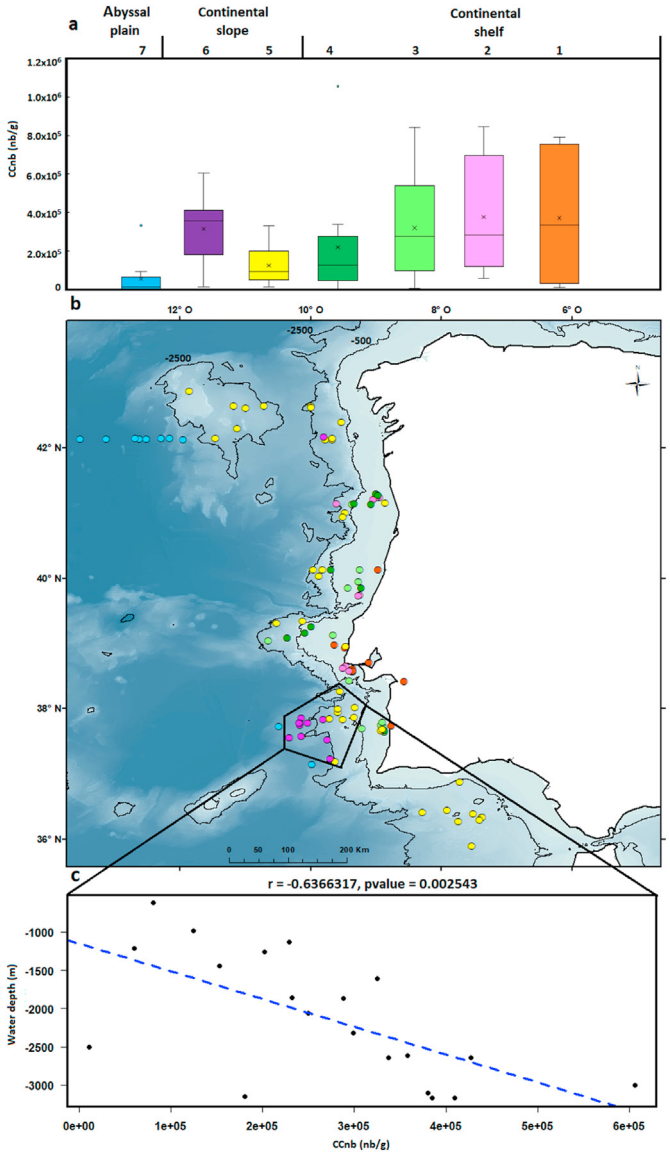

Fig. 8. Relationships between microcharcoal concentration and water depth. a) Boxplots representing the variability of microcharcoal concentration in seven groups defined by clustering analysis: samples located on the continental shelf (orange, pink, light green and dark green boxplots); samples located on the continental slope (yellow and purple boxplots); samples located in the abyssal plain (blue boxplot). b) Location of clusters. c) Scatter plot of microcharcoal concentrations and water depths for samples located in black polygon (Fig. 8b) and associated correlation coefficient. (For interpretation of the references to colour in this figure legend, the reader is referred to the Web version of this article.)

marine domain, while low values of these parameters in zones 1, 2 and 5 are associated with low mean microcharcoal concentrations (Fig. 6). Our results are in line with other studies suggesting that increases in microcharcoal concentration could be related with large fires of high intensity (Adolf et al., 2018; Duffin et al., 2008; Lynch et al., 2004). High-intensity fires consume more vegetation and thicker elements than leaves, such as twigs and branches (Higuera et al., 2005), producing more charcoals than low-intensity fires (Adolf et al., 2018; Duffin et al., 2008; Lynch et al., 2004). High fuel amount has also been suggested to explain high charcoal concentration in North American lakes and in marine surface sediments off the Pacific coast (Marlon et al., 2006; Smith et al., 1973). We hypothesise, therefore, that large infrequent fires of high intensity during dry summers produced the observed high amount of microscopic charcoal in zones 3 and 4.

Experimental analyses of length-to-width ratio of charcoal produced by the burning of "grass", "tree" and "shrub" species from North America, the United Kingdom and Arctic tundra showed that charcoal from "grass" has a greater elongation ratio than charcoal derived from "tree" and "shrub" (Umbanhowar and McGrath, 1998; Crawford and Belcher, 2014; Pereboom et al., 2020). Different elongation ratios are reported for grass and tree charcoal by these studies. For wood, a mean elongation ratio is about 2.13 ± 0.13 in muffle furnace or 2.23 ± 0.1 in open burn according to Umbanhowar and McGrath (1998) and about 1.97 according to Crawford and Belcher (2014). For grass, Crawford and Belcher (2014) observed a ratio of about 3.7, smaller than the ones observed by Umbanhowar and McGrath (1998) (3.62 ± 0.15 in muffle furnace and 4.83 + 0.27 in open burn), whereas Pereboom et al. (2020) reported a mean ratio of about 6.77. Our mean elongation ratios (between 1.43 and 2.96; Fig. 4c) in marine sediment samples are smaller compared to the ones from the experimental analyses. Smaller ratios may be linked to a higher breakage of charcoal particles due to the long transport by rivers.

However, boxplots of individual elongation values of microcharcoal show that zone 4 in particular presents a large amount of very elongated particles (outliers with an elongation ratio between 3 and 10) (Fig. 4d). Those values are close to the values obtained from experimental grass charcoal. In addition, Umbanhowar and McGrath (1998) reported that the elongation ratio is lower for particles trapped by a 125 μm versus a 250 μm sieve. Therefore, it is possible that our microcharcoal particles below 125 μm in length present globally smaller elongation ratios.

It is also likely that our samples consist of microcharcoal produced by different types of burnt vegetation and different species. Using relative changes in the mean elongation ratio therefore seems more relevant than using a threshold ratio to discriminate grass versus tree burnt-type vegetation between the different zones (Crawford and Belcher, 2014).

We suggest, therefore, that high microcharcoal concentrations in zones 3 and 4, marked by a large amount of elongated particles, reflect large and high intensity fires of low frequency spreading in open evergreen sclerophyllous Mediterranean forests (Fig. 1a), with an understorey composed of grasses. The low mean microcharcoal concentrations with a weak quantity of elongated particles in zones 1 and 5 would reflect small and low intensity fires of high frequency, spreading either in closed deciduous Atlantic forest for zone 1 (Figs. 1a and 7) or in open vegetation dominated by managed grass for zone 5 (Fig. 7). Although zones 2 and 3 present a similar proportion of burnt vegetation type, zone 2 is marked by a lower mean microcharcoal concentration and a weaker quantity of elongated particles compared to zones 3 and 4. This finding is in accordance with small and low intensity fires of high frequency (Fig. 6) occurring in the closed deciduous Atlantic forest (Fig. 1a). Mean microcharcoal concentrations and morphologies in marine sediments from the Iberian margin are then primarily controlled by the burnt vegetation type.

We suggest that the burning of open and mixed vegetation in zones 3 and 4 dominated by sclerophyllous vegetation produces more microcharcoal particles than the burning of closed vegetation in the northwestern Iberian Peninsula dominated by temperate trees. This is in agreement with the findings of Adolf et al. (2018) whose study showed higher microcharcoal accumulation in Mediterranean lake sediments than in lakes from temperate and boreal biome regions.

Our results suggest therefore high production of microcharcoal during the burning of open and mixed vegetation by intense fires under dry climate conditions (zones 3 and 4). However, similar

climate conditions in zone 5 are associated with frequent and small low intensity fires that occur in vegetation dominated by managed grasses. The low microcharcoal concentration is likely to be associated with the burning of this single type of vegetation, mostly post-harvest residues, as residence times of fire and fire intensities in grassland ecosystems are typically low (Johansen et al., 2001). Low microcharcoal concentration is also observed under wet climate conditions associated with small fires of low intensity in closed and mixed vegetation, limiting the amount of charcoal production (zones 1 and 2).

Based on 102 samples, our study further shows that microcharcoal concentration slightly decreases from the shelf to the upper slope (Fig. 8), then increases from the upper to the bottom slope, and decreases again in the abyssal plain. The distribution of microcharcoal particles in the ocean floor is independent of their shape (Fig. S11 and S12b), suggesting an homogeneous oceanic transport and deposition. The high variances within groups 1 to 4 reveal the large heterogeneity in the distribution of microcharcoal concentrations on the continental shelf (0–506 m bsl). This great heterogeneity may be due, as for the deposition of fine particles, to a high hydrodynamic environment with the action of the IPC and ICC ocean currents (Frouin et al., 1990; Villacieros-Robineau et al., 2019) and to the reworking of sediments during storms (Oliveira, 2002; van Weering et al., 2002). Naughton et al. (2007) observed a decreasing trend in pollen concentration from the shelf to the slope along the Iberian margin based on 10 surface samples. Our results suggest that microcharcoal transport in the marine realm is similar to that of pollen up to the upper slope. The increase of microcharcoal concentration along the slope is likely to be related to ocean sedimentation processes. The waves and hydrology effects on the shelf and on the upper slope during downwelling seasons (winter) lead to the remobilisation of fine particles inside bottom nepheloid layers, which accumulate in higher quantities in the middle and lower slopes in the northern part of the Iberian Peninsula (Dias Jouanneau et al., 2002; van Weering et al., 2002). In the south (in particular at the mouth of the Tagus) the remobilisation of fine particles inside bottom nepheloid layers during winter leads to the transport of sediments to the deep sea through canyons (Jouanneau et al., 1998).

The extremely low microcharcoal concentration in the abyssal plain (Group 7, between 3557 m and 3731 m bsl) (Fig. 8a) may be linked to a reduced transport and input of particles at locations far from the coast or to the settling/trapping of microcharcoal particles in sediments on the shelf and slope. This result is consistent with the one from Herring (1985) in the North Pacific, showing higher charcoal concentrations near land masses compared to open ocean sites at comparable latitudes, tentatively explained by river inputs and/or turbidite redeposition from shelf sediments. It is worth noting that microcharcoal concentration values from samples from the Gulf of Cádiz located at similar depths as the MOW are within the variability of group 5, suggesting that the MOW does not influence the deposition of microcharcoal in the Gulf of Cádiz.

5.2. Changes in southwestern iberia biomass burning during the Holocene

We used our present-day spatial relationships between microcharcoal concentration and environmental factors to infer changes in southwestern Iberia biomass burning during the Holocene from the microcharcoal record of core MD95-2042 located on the Portuguese margin off Lisbon (Daniau et al., 2007). Previous interpretation of this paleofire record suggested that low biomass burning associated with elongated particles during the cold phases of the last glacial period, Greenland Stadials (GS) and Heinrich Stadials (HS), were driven by a limited fuel grass environment, i.e. semi-desert vegetation composed of *Artemisia,* Chenopodiaceae and *Ephedra* (Daniau et al., 2007). During Greenland Interstadials (GI), the expansion of Mediterranean forests and heathlands (Ericaceae) increased fuel availability, leading to the increase in biomass burning (Daniau et al., 2007).

A long-term increase in microcharcoal concentrations (or influx) has been observed over the last 16,000 years (Fig. 9h). It is punctuated by a sharp trough between 12.9 and 11.8 kyr corresponding to the Younger Dryas (YD) and relatively low values between 10 and 8 kyr, both periods characterised by a high elongation ratio (Fig. 9g) (Daniau et al., 2007). From these data we infer the progressive increase of biomass burning during the deglaciation and the interglacial interrupted by two periods of burning decrease during the cold and dry YD and the warm and wet climatic optimum in the Iberian Peninsula (Chabaud et al., 2014; Gomes et al., 2020).

At present, the burning of open evergreen sclerophyllous Mediterranean vegetation in the Tagus and Sado watersheds produces higher microcharcoal concentration values (higher biomass burning) than in the closed Atlantic forests (Minho watershed) or in the mixed Atlantic and Mediterranean vegetation (Douro watershed) regions. Relatively high elongated particles are produced during the burning of open evergreen sclerophyllous Mediterranean vegetation (Tagus and Sado watersheds), of mixed Atlantic

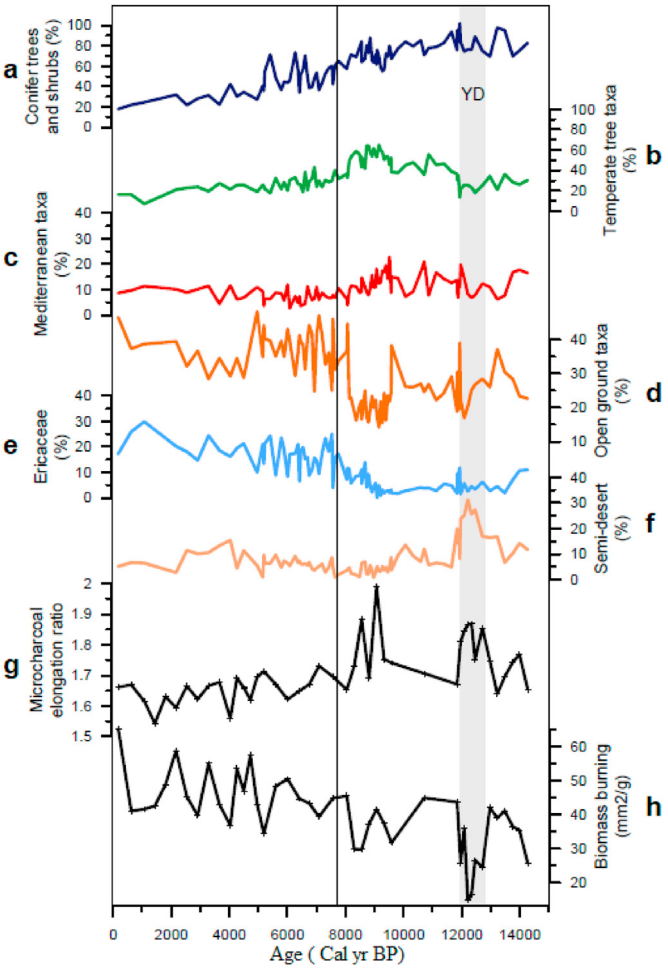

Fig. 9. Comparison between vegetation (a) to (f) and biomass burning (g) changes during the Holocene in the southwestern Iberian Peninsula recorded in the deep-sea core MD95-2042. Pollen percentages of (a) conifer trees and shrubs, (b) Temperate tree taxa, (c) Mediterranean taxa, (d) Open ground taxa, (e) Ericaceae, (f) Semi-desert (Chabaud et al., 2014), (g) Microcharcoal elongation ratio, (h) Microcharcoal concentrations (mm^2/g) (Daniau et al., 2007).

and Mediterranean vegetation (Douro watershed) and of open vegetation (Guadalquivir and Guadiana watersheds). Low elongation ratio characterised the Atlantic bioclimatic region dominated by deciduous forests and shrublands (Ericaceae) (Minho and Douro watersheds).

The sharp decrease of biomass burning, associated with elongated particles during the YD, and the relatively weak biomass burning between 10 and 8 kyr, suggest frequent small fires of low intensity occurring in open vegetation or in mixed Atlantic and evergreen sclerophyllous Mediterranean vegetations. The increase in microcharcoal concentrations during the past 8 kyr could have been driven by infrequent large fires of high intensity spreading into open evergreen sclerophyllous Mediterranean vegetation. However, the relatively low values of the elongation ratio suggest the burning of Atlantic vegetation and shrublands.

The comparison with pollen-based vegetation changes detected in the same core (Chabaud et al., 2014) confirms that the sharp decrease in biomass burning, associated with elongated particles during the YD, is associated with the expansion of semi-desert vegetation (Fig. 9f). The YD is characterised by cold and dry climate conditions in the area (Chabaud et al., 2014), potentially reducing fire hazards due to fire weather (less heat waves) or reducing fuel build-up associated with a fuel-limited environment of semi-desert vegetation (Gauquelin et al., 1998). Between 10 and 8 kyr, the relatively low biomass burning is associated with low percentages of open ground taxa (Fig. 9d) and with the development of evergreen sclerophyllous Mediterranean and temperate forests (Chabaud et al., 2014), a relatively closed Mediterranean forest rich in deciduous trees that are not fire-prone species (Fig. 9b and c). The new increase of biomass burning since 8 ka is associated with the expansion of open vegetation, mainly marked by the rise of Ericaceae-dominated shrublands (Fig. 9e) and open ground taxa and by the reduction of forest elements, i.e. a decrease in Mediterranean, temperate and conifer trees and shrubs (Fig. 9a), corresponding to the development of a maquis. Intense fires in Ericaceae shrublands produce high charcoal concentrations (Blackford, 2000). Ericaceae burning would also explain the relatively low values of the elongation ratio during this period, as observed in the Atlantic bioclimatic region at present. Our interpretation of biomass burning increase since 8 ka is in accordance with present-day plant and fire ecology. The opening of forests under disturbance, including fires, led to the expansion of shrubland/maquis communities including Ericaceae (Baudena et al., 2020; Le Houerou, 1973; Morales-Molino et al., 2020; Naughton et al., 2007).

6. Conclusion

Microscopic charcoal particles (between 10 and 125 μm-length) were analysed in 102 marine core-top sediment samples collected on the Iberian margin and the Gulf of Cádiz. Microcharcoal concentrations and morphologies (elongation) were quantified and compared to present-day satellite remote sensing fire patch information, climate and vegetation data, and physical site-specific variables on land and in the ocean, in order to better understand how microcharcoal concentrations represent fire regimes on land. Results show an increasing trend of microcharcoal concentrations from the north to the south of the Iberian margin, independent of the spatial pattern in the number of fires and the burnt areas. The spatial distribution of microcharcoal concentrations and morphologies may reflect patterns of fire size, fire radiative power, burnt vegetation type, climate, and NPP on land. We infer that increases of microcharcoal concentrations with a large amount of elongated particles are associated with rare and large summer fires of high intensity, fuelled during previous winters, spreading into open (shrub) vegetation under a hot and dry climate. Our results suggest that fires in open Mediterranean woodlands in the south of the Iberian Peninsula produce more microcharcoal than fires spreading in closed temperate forests in the north. No relationship was observed between the spatial distribution of concentrations and the physical site-specific variables on land (size of watershed, river discharges and suspended sediment loads). In the ocean, microcharcoal concentrations are highly variable on the continental shelf, increase along the slope and are low in the abyssal plain. The application of these results in the interpretation of a Holocene paleofire record from the Iberian margin, confirmed by the pollen-based vegetation record obtained from the same sample set, suggests that small and recurrent fires of low intensity were spreading in closed vegetation between 10–8 ka. In addition, large and rare fires of high intensity developed since 8 ka, contemporaneous with the degradation of the Mediterranean forest and the expansion of open (Ericaceae-dominated shrubland) vegetation.

Declaration of competing interest

The authors have no competing interests to declare.

Acknowledgements

This work was supported by the French INSU (Institut National des Sciences de l'Univers) programme LEFE (Les Enveloppes Fluides et l'Environnement) CAMPFIRE project; by the ANR BRAISE project, grant ANR-19-CE01-0001-01 of the French Agence Nationale de la Recherche; and by the ESA FIRECCI project. M. Genet is supported by a doctoral fellowship from the University of Bordeaux. We gratefully acknowledge I. Billy, O. Ther and L. Devaux for their technical help, and M. Rasolonjatovonirina for the initial burnt species data compilation. We thank EPOC and LSCE laboratories for giving us access to their repositories of marine sediments. We thank IFREMER for access to sediment cores curated at CREAM (Centre de Resources en Echantillons et Archives Marins) seabed sediment and rock samples repository. Particular thanks go to the staff from Unité de Recherche Géosciences Marines and from SISMER (French National Oceanographic Data Centre).

The authors are grateful to the chief scientists, coring and logistic teams of the CADISAR 1, CADISAR 2, FAEGAS 4, FORAMPROX-1, CEPAG, IMAGES V LEG5, JC089, OMEX 2, PACEMAKER, PALEO, PECH7, MD134-PICABIA, MD123-GEOSCIENCES 1, MD140-PRIVILEGE, MD141-ALIENOR 1, MD101-IMAGES 1 and NORES-TLANTE 3 leg 1 oceanographic cruises.

We thank Richard Vachula and two anonymous reviewers for their valuable comments.

Author contributions

M.G. and A.-L.D. designed research; M.G. performed research; F.M.,V.H., S.S., V.D., M.G., F.A., P.A., F.B., J.B., B.D., F.E., D.A.H., T.M., F.N., L.R., P.T., M.F.S.G. contributed data, analytic advices and sediments; M.G and A.-L.D led the writing of the paper. All authors edited the paper.

Appendix A. Supplementary data

Supplementary data to this article can be found online at https://doi.org/10.1016/j.quascirev.2021.107148.

References

Adolf, C., Wunderle, S., Colombaroli, D., Weber, H., Gobet, E., Heiri, O., Leeuwen, J.F.N., van Bigler, C., Connor, S.E., Gałka, M., Mantia, T.L., Makhortykh, S., Svitavská-Svobodová, H., Vannière, B., Tinner, W., 2018. The

sedimentary and remote-sensing reflection of biomass burning in Europe. Global Ecol. Biogeogr. 27, 199–212. https://doi.org/10.1111/geb.12682.
Alcara Ariza, F., Asensi Marfil, A., de Bolos y Capdevilla, O., Costa Tales, M., Arco Aguilar, M., Diaz Gonzales, T.E., Diez Garretas, B., Fernandez Prieto, J.A., Fernandez Gonzales, F., Izco Sevillando, J., Loidi Arregui, J., Martinez Parras, J.M., Navarro Andres, F., Ninot I Sugranes, J.M., Peinado Lorca, M., Rivas Martinez, S., Sanchez Mata, D., Valle Guitierrez, C., Vigo I Bonada, J., Wildpret de la Torre, W., 1992. La vegetacion de España [WWW Document].
Almeida, P.R., 2003. Feeding ecology of Liza ramada (Risso, 1810) (Pisces, Mugilidae) in a south-western estuary of Portugal. Estuarine. Coastal and Shelf Science 57, 313–323. https://doi.org/10.1016/S0272-7714(02)00357-8.
Alves, T., 2003. Cenozoic tectono-sedimentary evolution of the western Iberian margin. Mar. Geol. 195, 75–108. https://doi.org/10.1016/S0025-3227(02)00683-7.
Archibald, S., Lehmann, C.E.R., Belcher, C.M., Bond, W.J., Bradstock, R.A., Daniau, A.-L., Dexter, K.G., Forrestel, E.J., Greve, M., He, T., Higgins, S.I., Hoffmann, W.A., Lamont, B.B., McGlinn, D.J., Moncrieff, G.R., Osborne, C.P., Pausas, J.G., Price, O., Ripley, B.S., Rogers, B.M., Schwilk, D.W., Simon, M.F., Turetsky, M.R., Van der Werf, G.R., Zanne, A.E., 2018. Biological and geophysical feedbacks with fire in the Earth system. Environ. Res. Lett. 13. https://doi.org/10.1088/1748-9326/aa9ead, 033003.
Baudena, M., Santana, V.M., Baeza, M.J., Bautista, S., Eppinga, M.B., Hemerik, L., Mayor, A.G., Rodriguez, F., Valdecantos, A., Vallejo, V.R., Vasques, A., Rietkerk, M., 2020. Increased aridity drives post-fire recovery of Mediterranean forests towards open shrublands. New Phytol. 225, 1500–1515. https://doi.org/10.1111/nph.16252.
Beaufort, L., de Garidel-Thoron, T., Linsley, B., Oppo, D., Buchet, N., 2003. Biomass burning and oceanic primary production estimates in the Sulu Sea area over the last 380 kyr and the East Asian monsoon dynamics. Mar. Geol. 201, 53–65. https://doi.org/10.1016/S0025-3227(03)00208-1.
Blackford, J.J., 2000. Charcoal fragments in surface samples following a fire and the implications for interpretation of subfossil charcoal data. Palaeogeogr. Palaeoclimatol. Palaeoecol. 164, 33–42. https://doi.org/10.1016/S0031-0182(00)00173-5.
Blanco-Castro, B., Casado González, E., Costa Tenorio, M.A., Escribano Bombín, M., García Antón, R., Génova Fuster, M., 1997. Los bosques IBERICOS: una INTERPETACION GEOBOTANICA. GeoPlaneta 572.
Boulter, M.C., 1994. An approach to a standard terminology for palynodebris. In: Traverse, A. (Ed.), Sedimentation of Organic Particles. Cambridge University Press, Cambridge, pp. 199–216.
Bowman, D.M.J.S., Balch, J.K., Artaxo, P., Bond, W.J., Carlson, J.M., Cochrane, M.A., D'Antonio, C.M., DeFries, R.S., Doyle, J.C., Harrison, S.P., Johnston, F.H., Keeley, J.E., Krawchuk, M.A., Kull, C.A., Marston, J.B., Moritz, M.A., Prentice, I.C., Roos, C.I., Scott, A.C., Swetnam, T.W., van der Werf, G.R., Pyne, S.J., 2009. Fire in the earth system. Science 324, 481–484. https://doi.org/10.1126/science.1163886.
Cardil, A., Molina, D.M., Kobziar, L.N., 2014. Extreme temperature days and their potential impacts on southern Europe. Nat. Hazards Earth Syst. Sci. 14, 3005–3014. https://doi.org/10.5194/nhess-14-3005-2014.
Carmona-Moreno, C., Belward, A., Malingreau, J.-P., Hartley, A., Garcia-Alegre, M., Antonovskiy, M., Buchshtaber, V., Pivovarov, V., 2005. Characterizing interannual variations in global fire calendar using data from Earth observing satellites. Global Change Biol. 11, 1537–1555. https://doi.org/10.1111/j.1365-2486.2005.01003.x.
Chabaud, L., Sánchez Goñi, M.F., Desprat, S., Rossignol, L., 2014. Land–sea climatic variability in the eastern North Atlantic subtropical region over the last 14,200 years: atmospheric and oceanic processes at different timescales. Holocene 24, 787–797. https://doi.org/10.1177/0959683614530439.
Clark, J.S., 1988. Particle motion and the theory of charcoal analysis: source area, transport, deposition, and sampling. Quat. Res. 30, 67–80. https://doi.org/10.1016/0033-5894(88)90088-9.
Conedera, M., Tinner, W., Neff, C., Meurer, M., Dickens, A.F., Krebs, P., 2009. Reconstructing past fire regimes: methods, applications, and relevance to fire management and conservation. Quat. Sci. Rev. 28, 555–576. https://doi.org/10.1016/j.quascirev.2008.11.005.
Couso-Pérez, S., Cañizo-Outeiriño, A., Campo-Ramos, R., Ares-Mazás, E., Gómez-Couso, H., 2018. Remarkable differences in the presence of the acanthocephalan parasite Echinorhynchus truttae in brown trout (Salmo trutta) captured in two adjacent river basins in Galicia (NW Spain). Parasitology Open 4, e5. https://doi.org/10.1017/pao.2017.24.
Crawford, A.J., Belcher, C.M., 2014. Charcoal morphometry for paleoecological analysis: the effects of fuel type and transportation on morphological parameters. Applications in Plant Sciences 2 (1400004). https://doi.org/10.3732/apps.1400004.
Crous-Duran, J., Paulo, J.A., Palma, J.H.N., 2014. Montado in Portugal. High Natural and Cultural Value Agroforestry, in: Initial Stakeholder Meeting Report. Montado in Portugal.
Daniau, A.-L., Sánchez-Goñi, M.F., Beaufort, L., Laggoun-Défarge, F., Loutre, M.-F., Duprat, J., 2007. Dansgaard–Oeschger climatic variability revealed by fire emissions in southwestern Iberia. Quat. Sci. Rev. 26, 1369–1383. https://doi.org/10.1016/j.quascirev.2007.02.005.
Daniau, A.-L., Harrison, S.P., Bartlein, P.J., 2010. Fire regimes during the last glacial. Quat. Sci. Rev. 29, 2918–2930. https://doi.org/10.1016/j.quascirev.2009.11.008.
Daniau, A.-L., Desprat, S., Aleman, J.C., Bremond, L., Davis, B., Fletcher, W., Marlon, J.R., Marquer, L., Montade, V., Morales-Molino, C., Naughton, F., Rius, D., Urrego, D.H., 2019. Terrestrial plant microfossils in palaeoenvironmental studies, pollen, microcharcoal and phytolith. Towards a comprehensive understanding of vegetation, fire and climate changes over the past one million years. Rev. Micropaleontol. 63, 1–35. https://doi.org/10.1016/j.revmic.2019.02.001.
de Bar, M.W., Weiss, G., Yildiz, C., Rampen, S.W., Lattaud, J., Bale, N.J., Mienis, F., Brummer, G.-J.A., Schulz, H., Rush, D., Kim, J.-H., Donner, B., Knies, J., Lückge, A., Stuut, J.-B.W., Sinninghe Damsté, J.S., Schouten, S., 2020. Global temperature calibration of the Long chain Diol Index in marine surface sediments. Org. Geochem. 142 (103983). https://doi.org/10.1016/j.orggeochem.2020.103983.
Dessandier, P.-A., Bonnin, J., Kim, J.-H., Bichon, S., Deflandre, B., Grémare, A., Sinninghe Damsté, J.S., 2016. Impact of organic matter source and quality on living benthic foraminiferal distribution on a river-dominated continental margin: a study of the Portuguese margin: benthic foraminifera. J. Geophys. Res. Biogeosci 121, 1689–1714. https://doi.org/10.1002/2015JG003231.
Dias, J., 1987. Dinâmica sedimentar e evolução recente daplataforma continental portuguesa setentrional. PhD thesis. Univ. Lisbon 384.
Dias Jouanneau, J.M., Gonzalez, R., Araújo, M.F., Drago, T., Garcia, C., Oliveira, A., Rodrigues, A., Vitorino, J. Weber O., 2002. Present day sedimentary processes on the northern Iberian shelf. Progress in Oceanography, Benthic processes and dynamics at the NW Iberian Margin. resultss of the OMEX II Program 52, 249–259. https://doi.org/10.1016/S0079-6611(02)00009-5.
Droogers, P., Immerzeel, W., 2008. Water Resources Guadalquivir basin, Spain.
Duffin, K.I., Gillson, L., Willis, K.J., 2008. Testing the sensitivity of charcoal as an indicator of fire events in savanna environments: quantitative predictions of fire proximity, area and intensity. Holocene 18, 279–291. https://doi.org/10.1177/0959683607086766.
Dupont, L., Wyputta, U., 2003. Reconstructing pathways of aeolian pollen transport to the marine sediments along the coastline of SW Africa. Quat. Sci. Rev. 22, 157–174. https://doi.org/10.1016/S0277-3791(02)00032-X.
Fernández-Delgado, C., Baldó, F., Vilas, C., García-González, D., Cuesta, J.A., González-Ortegón, E., Drake, P., 2007. Effects of the river discharge management on the nursery function of the Guadalquivir river estuary (SW Spain). Hydrobiologia 587, 125–136. https://doi.org/10.1007/s10750-007-0691-9.
Fernández-Nogueira, D., Corbelle-Rico, E., 2018. Land use changes in iberian Peninsula 1990–2012. https://doi.org/10.3390/land7030099. Land, 7,99.
Ferreira, V., Graça, M.A.S., Feio, M.J., Mieiro, C., 2004. Water quality in the Mondego river basin: pollution and habitat heterogeneity 12.
Frouin, R., Fiúza, A.F.G., Ambar, I., Boyd, T.J., 1990. Observations of a poleward surface current off the coasts of Portugal and Spain during winter. J. Geophys. Res. 95 (679). https://doi.org/10.1029/JC095iC01p00679.
Garel, E., Pinto, L., Santos, A., Ferreira, Ó., 2009. Tidal and river discharge forcing upon water and sediment circulation at a rock-bound estuary (Guadiana estuary, Portugal). Estuarine. Coastal and Shelf Science 84, 269–281. https://doi.org/10.1016/j.ecss.2009.07.002.
Gauquelin, T., Jalut, G., Iglesias, M., 1998. Phytomass and carbon storage in the steppes of Eastern Andalusia, Spain. Ambio (Sweden) (Granada U. (Spain) D. de B.V., Valle, F.
Giglio, L., Randerson, J.T., Werf, G.R. van der, 2013. Analysis of daily, monthly, and annual burned area using the fourth-generation global fire emissions database (GFED4). J. Geophys. Res.: Biogeosciences 118, 317–328. https://doi.org/10.1002/jgrg.20042.
Gomes, S.D., Fletcher, W.J., Rodrigues, T., Stone, A., Abrantes, F., Naughton, F., 2020. Time-transgressive Holocene maximum of temperate and Mediterranean forest development across the Iberian Peninsula reflects orbital forcing. Palaeogeography, Palaeoclimatology. Palaeoecology 550 (109739). https://doi.org/10.1016/j.palaeo.2020.109739.
Gonçalves, A.C., Sousa, A.M.O., 2017. The fire in the mediterranean region: a case study of forest fires in Portugal. In: Fuerst-Bjelis, B. (Ed.), Mediterranean Identities - Environment, Society, Culture. InTech. https://doi.org/10.5772/intechopen.69410.
Grolier online Atlas, 2021. http://go.grolier.com/atlas?id=mtsp009&tn=/atlas/nec2/printerfriendly.html.
Guerreiro, C., Rodrigues, A., Duarte, J., Oliveira, A., Taborda, R., 2007. Bottom sediment signature associated with the oporto, aveiro and nazaré submarine canyons (NW OFF Portugal) 11.
Guerreiro, C., de Stigter, H., Cachão, M., Oliveira, A., Rodrigues, A., 2015. Coccoliths from recent sediments of the central Portuguese margin: taphonomical and ecological inferences. Mar. Micropaleontol. 114, 55–68. https://doi.org/10.1016/j.marmicro.2014.11.001.
Guerreiro, S.B., Birkinshaw, S., Kilsby, C., Fowler, H.J., Lewis, E., 2017. Dry getting drier – the future of transnational river basins in Iberia. J. Hydrol.: Reg. Stud. 12, 238–252. https://doi.org/10.1016/j.ejrh.2017.05.009.
Habib, D., Eshet, Y., Pelt, R., 1994. Sedimentation of organic particles: palynology of sedimentary cycles. https://doi.org/10.1017/CBO9780511524875.017.
Hall, J.R., 2014. The total cost of fire in the United States. In: National Fire Protection Association Quincy, MA.
Hammer, O., Harper, D.A.T., Ryan, P.D., 2000. PAST: paleontological statistics software package for education and data analysis 9.
Hantson, S., Arneth, A., Harrison, S.P., Kelley, D.I., Prentice, I.C., Rabin, S.S., Archibald, S., Mouillot, F., Arnold, S.R., Artaxo, P., Bachelet, D., Ciais, P., Forrest, M., Friedlingstein, P., Hickler, T., Kaplan, J.O., Kloster, S., Knorr, W., Lasslop, G., Li, F., Mangeon, S., Melton, J.R., Meyn, A., Sitch, S., Spessa, A., 2016. The status and challenge of global fire modelling 19.
Hart, G.F., Pasley, M.A., Gregory, W.A., 1994. Sequence stratigraphy and

sedimentation of organic particles. In: Traverse, A. (Ed.), Sedimentation of Organic Particles. Cambridge University Press, Cambridge, pp. 337–390.
Hawthorne, D., Courtney Mustaphi, C.J., Aleman, J.C., Blarquez, O., Colombaroli, D., Daniau, A.-L., Marlon, J.R., Power, M., Vannière, B., Han, Y., Hantson, S., Kehrwald, N., Magi, B., Yue, X., Carcaillet, C., Marchant, R., Ogunkoya, A., Githumbi, E.N., Muriuki, R.M., 2018. Global Modern Charcoal Dataset (GMCD): a tool for exploring proxy-fire linkages and spatial patterns of biomass burning. Quat. Int. 488, 3–17. https://doi.org/10.1016/j.quaint.2017.03.046.
Hernández-Molina, F.J., Serra, N., Stow, D.A.V., Llave, E., Ercilla, G., Van Rooij, D., 2011. Along-slope oceanographic processes and sedimentary products around the Iberian margin. Geo Mar. Lett. 31, 315–341. https://doi.org/10.1007/s00367-011-0242-2.
Herring, J.R., 1985. Charcoal fluxes into sediments of the North Pacific Ocean: the Cenozoic record of burning. The carbon cycle and atmospheric CO2: natural variations Archean to present 32, 419–442.
Heusser, L., Balsam, W.L., 1977. Pollen distribution in the northeast pacific ocean. Quat. res 7, 45–62. https://doi.org/10.1016/0033-5894(77)90013-8.
Higuera, P.E., Sprugel, D.G., Brubaker, L.B., 2005. Reconstructing fire regimes with charcoal from small-hollow sediments: a calibration with tree-ring records of fire. Holocene 15, 238–251. https://doi.org/10.1191/0959683605hl789rp.
Hockaday, W.C., Grannas, A.M., Kim, S., Hatcher, P.G., 2006. Direct molecular evidence for the degradation and mobility of black carbon in soils from ultrahigh-resolution mass spectral analysis of dissolved organic matter from a fire-impacted forest soil. Org. Geochem. 37, 501–510. https://doi.org/10.1016/j.orggeochem.2005.11.003.
Hooghiemstra, H., Stalling, H., Agwu, C.O.C., Dupont, L.M., 1992. Vegetational and climatic changes at the northern fringe of the Sahara 250,000-5000 years BP: evidence from 4 marine pollen records located between Portugaland the Canary Islands.Rev. Palaeobot. Palynol.74 1–53. https://doi.org/10.1016/0034-6667(92)90137-6.
Hooghiemstra, H., Lézine, A.-M., Leroy, S.A.G., Dupont, L., Marret, F., 2006. Late Quaternary palynology in marine sediments: a synthesis of the understanding of pollen distribution patterns in the NW African setting. Quat. Int. 148, 29–44. https://doi.org/10.1016/j.quaint.2005.11.005.
Johansen, M.P., Hakonson, T.E., Breshears, D.D., 2001. Post-fire runoff and erosion from rainfall simulation: contrasting forests with shrublands and grasslands. Hydrol. Process. 15, 2953–2965. https://doi.org/10.1002/hyp.384.
Jouanneau, J.M., Garcia, C., Oliveira, A., Rodrigues, A., Dias, J.A., Weber, O., 1998. Dispersal and deposition of suspended sediment on the shelf off the Tagus and Sado estuaries, S.W. Portugal. Prog. Oceanogr. 42, 233–257. https://doi.org/10.1016/S0079-6611(98)00036-6.
Jouanneau, J.M., Weber, O., Drago, T., Rodrigues, A., Oliveira, A., Dias, J.M.A., Garcia, C., Schmidt, S., Reyss, J.L., 2002. Recent sedimentation and sedimentary budgets on the western Iberian shelf. Progress in Oceanography, Benthic processes and dynamics at the NW Iberian Margin: resultss of the OMEX II Program 52, 261–275. https://doi.org/10.1016/S0079-6611(02)00010-1.
Kalnay, E., Kanamitsu, M., Kistler, R., Collins, W., Deaven, D., Gandin, L., Iredell, M., Saha, S., White, G., Woollen, J., Zhu, Y., Chelliah, M., Ebisuzaki, W., Higgins, W., Janowiak, J., Mo, K.C., Ropelewski, C., Wang, J., Leetmaa, A., Reynolds, R., Jenne, R., Joseph, D., 1996. The NCEP/NCAR 40-Year Reanalysis Project. Bull. Am. Meteorol. Soc. 77, 437–472. https://doi.org/10.1175/1520-0477(1996)077<0437:TNYRP>2.0.CO;2.
Kim, J.-H., Schouten, S., Hopmans, E.C., Donner, B., Sinninghe Damsté, J.S., 2008. Global sediment core-top calibration of the TEX86 paleothermometer in the ocean. Geochem. Cosmochim. Acta 72, 1154–1173. https://doi.org/10.1016/j.gca.2007.12.010.
Kondolf, G.M., Gao, Y., Annandale, G.W., Morris, G.L., Jiang, E., Zhang, J., Cao, Y., Carling, P., Fu, K., Guo, Q., Hotchkiss, R., Peteuil, C., Sumi, T., Wang, H.-W., Wang, Z., Wei, Z., Wu, B., Wu, C., Yang, C.T., 2014. Sustainable sediment management in reservoirs and regulated rivers: experiences from five continents. Earth's Future 2, 256–280. https://doi.org/10.1002/2013EF000184.
Krebs, P., Pezzatti, G.B., Mazzoleni, S., Talbot, L.M., Conedera, M., 2010. Fire regime: history and definition of a key concept in disturbance ecology. Theor. Biosci. 129, 53–69. https://doi.org/10.1007/s12064-010-0082-z.
Kucera, M., Weinelt, Mara, Kiefer, T., Pflaumann, U., Hayes, A., Weinelt, Martin, Chen, M.-T., Mix, A.C., Barrows, T.T., Cortijo, E., Duprat, J., Juggins, S., Waelbroeck, C., 2005. Reconstruction of sea-surface temperatures from assemblages of planktonic foraminifera: multi-technique approach based on geographically constrained calibration data sets and its application to glacial Atlantic and Pacific Oceans. Quat. Sci. Rev. 24, 951–998. https://doi.org/10.1016/j.quascirev.2004.07.014.
Lastras, G., Arzola, R.G., Masson, D.G., Wynn, R.B., Huvenne, V.A.I., Hühnerbach, V., Canals, M., 2009. Geomorphology and sedimentary features in the Central Portuguese submarine canyons, Western Iberian margin. Geomorphology 103, 310–329. https://doi.org/10.1016/j.geomorph.2008.06.013.
Laurent, P., Mouillot, F., Yue, C., Ciais, P., Moreno, M.V., Nogueira, J.M.P., 2018. FRY, a global database of fire patch functional traits derived from space-borne burned area products. Sci Data 5 (180132). https://doi.org/10.1038/sdata.2018.132.
Laurent, P., Mouillot, F., Moreno, M.V., Yue, C., Ciais, P., 2019. Varying relationships between fire radiative power and fire size at a global scale. Biogeosciences 16, 275–288. https://doi.org/10.5194/bg-16-275-2019.
Lê, S., Josse, J., Husson, F., 2008. FactoMineR : an *R* package for multivariate analysis. J. Stat. Software 25. https://doi.org/10.18637/jss.v025.i01.
Le Houerou, H.N., 1973. Fire and vegetation in the Mediterranean basin 41.
Lebreiro, S.M., Nicholas, M.C.C., I Weaver, P.P.E., 1997. Late quaternary turbidite emplacement on the horseshoe abyssal plain (iberian margin). SEPM JSR 67. https://doi.org/10.1306/D4268658-2B26-11D7-8648000102C1865D.
Lehner, B., Liermann, C.R., Revenga, C., Vörösmarty, C., Fekete, B., Crouzet, P., Döll, P., Endejan, M., Frenken, K., Magome, J., Nilsson, C., Robertson, J.C., Rödel, R., Sindorf, N., Wisser, D., 2011. High-resolution mapping of the world's reservoirs and dams for sustainable river-flow management. Front. Ecol. Environ. 9, 494–502. https://doi.org/10.1890/100125.
Leys, B., Brewer, S.C., McConaghy, S., Mueller, J., McLauchlan, K.K., 2015. Fire history reconstruction in grassland ecosystems: amount of charcoal reflects local area burned. Environ. Res. Lett. 10 (114009). https://doi.org/10.1088/1748-9326/10/11/114009.
Liu, Y., Stanturf, J., Goodrick, S., 2010. Trends in global wildfire potential in a changing climate. For. Ecol. Manag. 259, 685–697. https://doi.org/10.1016/j.foreco.2009.09.002.
Lobo, F.J., Hernández-Molina, F.J., Somoza, L., Diaz del Rio, V., 2001. The sedimentary record of the post-glacial transgression on the Gulf of Cadiz continental shelf (Southwest Spain). Mar. Geol. 178, 171–195. https://doi.org/10.1016/S0025-3227(01)00176-1.
Lohman, D.J., Bickford, D., Sodhi, N.S., 2007. ENVIRONMENT: the burning issue. Science 316. https://doi.org/10.1126/science.1140278, 376–376.
Lynch, J.A., Clark, J.S., Stocks, B.J., 2004. Charcoal production, dispersal, and deposition from the Fort Providence experimental fire: interpreting fire regimes from charcoal records in boreal forests 34, 15.
Maestro, A., López-Martínez, J., Llave, E., Bohoyo, F., Acosta, J., Hernández-Molina, F.J., Muñoz, A., Jané, G., 2013. Geomorphology of the iberian continental margin. Geomorphology 196, 13–35. https://doi.org/10.1016/j.geomorph.2012.08.022.
Marlon, J., Bartlein, P.J., Whitlock, C., 2006. Fire-fuel-climate linkages in the northwestern USA during the Holocene. Holocene 16, 1059–1071. https://doi.org/10.1177/0959683606069396.
Marlon, J.R., Kelly, R., Daniau, A.-L., Vannière, B., Power, M.J., Bartlein, P., Higuera, P., Blarquez, O., Brewer, S., Brücher, T., Feurdean, A., Romera, G.G., Iglesias, V., Maezumi, S.Y., Magi, B., Courtney Mustaphi, C.J., Zhihai, T., 2016. Reconstructions of biomass burning from sediment-charcoal records to improve data–model comparisons. Biogeosciences 13, 3225–3244. https://doi.org/10.5194/bg-13-3225-2016.
Marta, P., Bochechas, J., Collares-Pereira, M.J., 2001. Importance of recreational fisheries in the Guadiana river basin in Portugal. Fish. Manag. Ecol. 8, 345–354. https://doi.org/10.1111/j.1365-2400.2001.00262.x.
Mensing, S.A., Michaelsen, J., Byrne, R., 1999. A 560-year record of santa ana fires reconstructed from charcoal deposited in the santa barbara basin, California. Quat. Res. 51, 295–305. https://doi.org/10.1006/qres.1999.2035.
Mil-Homens, M., Vale, C., Raimundo, J., Pereira, P., Brito, P., Caetano, M., 2014. Major factors influencing the elemental composition of surface estuarine sediments: the case of 15 estuaries in Portugal. Mar. Pollut. Bull. 84, 135–146. https://doi.org/10.1016/j.marpolbul.2014.05.026.
Millspaugh, S.H., Whitlock, C., 1995. A 750-year fire history based on lake sediment records in central Yellowstone National Park, USA. Holocene 5, 283–292. https://doi.org/10.1177/095968369500500303.
Morales-Molino, C., Devaux, L., Georget, M., Hanquiez, V., Sánchez Goñi, M.F., 2020. Modern pollen representation of the vegetation of the Tagus basin (central iberian Peninsula). Rev. Palaeobot. Palynol. 276 (104193). https://doi.org/10.1016/j.revpalbo.2020.104193.
Moriondo, M., Good, P., Durao, R., Bindi, M., Giannakopoulos, C., Corte-Real, J., 2006. Potential impact of climate change on fire risk in the Mediterranean area. Clim. Res. 31, 85–95. https://doi.org/10.3354/cr031085.
Mougenot, D., Vanney, J., 1982. Les rides de CONTOURITES plio-QUATERNAIRES de la pente continentale sud-PORTUGAISE.
Mouillot, F., Rambal, S., Joffre, R., 2002. Simulating climate change impacts on fire frequency and vegetation dynamics in a Mediterranean-type ecosystem. Global Change Biol. 8, 423–437. https://doi.org/10.1046/j.1365-2486.2002.00494.x.
Mouillot, F., Ratte, J.-P., Joffre, R., Mouillot, D., Serge, Rambal, 2005. Long-term forest dynamic after land abandonment in a fire prone Mediterranean landscape (central Corsica, France). Landsc. Ecol. 20, 101–112. https://doi.org/10.1007/s10980-004-1297-5.
Mouillot, F., Schultz, M.G., Yue, C., Cadule, P., Tansey, K., Ciais, P., Chuvieco, E., 2014. Ten years of global burned area products from spaceborne remote sensing—a review: analysis of user needs and recommendations for future developments. Int. J. Appl. Earth Obs. Geoinf. 26, 64–79. https://doi.org/10.1016/j.jag.2013.05.014.
Mudie, P.J., 1982. Pollen distribution in recent marine sediments, eastern Canada. Can. J. Earth Sci. 19, 729–747. https://doi.org/10.1139/e82-062.
Mudie, P.J., McCarthy, F.M.G., 2006. Marine palynology: potentials for onshore—offshore correlation of Pleistocene—Holocene records. Trans. Roy. Soc. S. Afr. 61, 139–157. https://doi.org/10.1080/00359190609519964.
Müller, P.J., Kirst, G., Ruhland, G., von Storch, I., Rosell-Melé, A., 1998. Calibration of the alkenone paleotemperature index U37K′ based on core-tops from the eastern South Atlantic and the global ocean (60°N-60°S). Geochem. Cosmochim. Acta 62, 1757–1772. https://doi.org/10.1016/S0016-7037(98)00097-0.
Naughton, F., Sanchez Goñi, M.F., Desprat, S., Turon, J.-L., Duprat, J., Malaizé, B., Joli, C., Cortijo, E., Drago, T., Freitas, M.C., 2007. Present-day and past (last 25000

years) marine pollen signal off western Iberia. Mar. Micropaleontol. 62, 91–114. https://doi.org/10.1016/j.marmicro.2006.07.006.
New, M., Lister, D., Hulme, M., Makin, I., 2002. A high-resolution data set of surface climate over global land areas. Clim. Res. 21, 1–25. https://doi.org/10.3354/cr021001.
Oliveira, I.B.M., 2002. Littoral problems IN the Portuguese west coast 20.
Oliveira, A., Rodrigues, A., Jouanneau, J.M., Weber, O., Alveirinho-Dias, J.M., Vitorino, J., 1999. Suspended particulate matter distribution and composition on the northern Portuguese margin 9.
Otero, P., Ruiz-Villarreal, M., García-García, L., González-Nuevo, G., Cabanas, J.M., 2013. Coastal dynamics off Northwest Iberia during a stormy winter period. Ocean Dynam. 63, 115–129. https://doi.org/10.1007/s10236-012-0585-x.
Patterson, W.A., Edwards, K.J., Maguire, D.J., 1987. Microscopic charcoal as a fossil indicator of fire. Quat. Sci. Rev. 6, 3–23. https://doi.org/10.1016/0277-3791(87)90012-6.
Pausas, J.G., Paula, S., 2012. Fuel shapes the fire–climate relationship: evidence from Mediterranean ecosystems. Global Ecol. Biogeogr. 21, 1074–1082. https://doi.org/10.1111/j.1466-8238.2012.00769.x.
Pechony, O., Shindell, D.T., 2010. Driving forces of global wildfires over the past millennium and the forthcoming century. Proc. Natl. Acad. Sci. Unit. States Am. 107, 19167–19170. https://doi.org/10.1073/pnas.1003669107.
Pereboom, E.M., Vachula, R.S., Huang, Y., Russell, J., 2020. The morphology of experimentally produced charcoal distinguishes fuel types in the Arctic tundra. Holocene 30, 1091–1096. https://doi.org/10.1177/0959683620908629.
Polunin, O., Walters, M., 1985. A Guide to the Vegetation of Britain and Europe. Oxford University Press, New York, p. 238.
Portela, L.I., 2008. Sediment transport and morphodynamics of the Douro River estuary. Geo Mar. Lett. 28, 77–86. https://doi.org/10.1007/s00367-007-0091-1.
Poulter, B., MacBean, N., Hartley, A., Khlystova, I., Arino, O., Betts, R., Bontemps, S., Boettcher, M., Brockmann, C., Defourny, P., Hagemann, S., Herold, M., Kirches, G., Lamarche, C., Lederer, D., Ottlé, C., Peters, M., Peylin, P., 2015. Plant functional type classification for earth system models: results from the European Space Agency's Land Cover Climate Change Initiative. Geosci. Model Dev. (GMD) 8, 2315–2328. https://doi.org/10.5194/gmd-8-2315-2015.
Pugnet, L., Lourenço, L., Rocha, J., 2010. L'IGNITION des feux de forêt par L'ACTION de la foudre au Portugal de 1996 à 2008 14.
Quénéa, K., Derenne, S., Rumpel, C., Rouzaud, J.-N., Gustafsson, O., Carcaillet, C., Mariotti, A., Largeau, C., 2006. Black carbon yields and types in forest and cultivated sandy soils (Landes de Gascogne, France) as determined with different methods: influence of change in land use. Org. Geochem. 37, 1185–1189. https://doi.org/10.1016/j.orggeochem.2006.05.010.
Radi, T., de Vernal, A., 2008. Dinocysts as proxy of primary productivity in mid–high latitudes of the Northern Hemisphere. Mar. Micropaleontol. 68, 84–114. https://doi.org/10.1016/j.marmicro.2008.01.012.
Rhodes, A.N., 1998. A method for the preparation and quantification of microscopic charcoal from terrestrial and lacustrine sediment cores. Holocene 8, 113–117. https://doi.org/10.1191/095968398671104653.
Robinne, F.-N., Burns, J., Kant, P., Flannigan, M., Kleine, M., de Groot, B., Wotton, D.M., 2018. Global fire challenges in a warming world. IUFRO.
Rodrigues, M., Trigo, R.M., Vega-García, C., Cardil, A., 2020. Identifying large fire weather typologies in the Iberian Peninsula. Agric. For. Meteorol. 280 (107789). https://doi.org/10.1016/j.agrformet.2019.107789.
Ruffault, J., Curt, T., Moron, V., Trigo, R.M., Mouillot, F., Koutsias, N., Pimont, F., Martin-StPaul, N.K., Barbero, R., Dupuy, J.-L., Russo, A., Belhadj-Kheder, C., 2020. Increased likelihood of heat-induced large wildfires in the Mediterranean Basin. bioRxiv 2020.01.09.896878. https://doi.org/10.1101/2020.01.09.896878.
Running, S.W., Thornton, P.E., Nemani, R., Glassy, J.M., 2000. Global Terrestrial Gross and Net Primary Productivity from the Earth Observing System. In: Sala, O.E., Jackson, R.B., Mooney, H.A., Howarth, R.W. (Eds.), Methods in Ecosystem Science. Springer New York, New York, NY, pp. 44–57. https://doi.org/10.1007/978-1-4612-1224-9_4.
San-miguel-ayanz, J., Durrant, T., Boca, R., Libertá, G., Branco, A., Rigo, D., Ferrari, D., Maianti, P., Vivancos, T.A., Costa, H., Lana, F., Loffler, P., Nujiten, D., Ahlgren, A.C., Leray, T., 2018. Forest fires in Europe, Middle East and north africa 2017. Publications Office 139.
Sanchez, P.J., 2007. Fundamentals OF simulation modeling 9.
Schmidt, S., de Stigter, H.C., van Weering, T.C.E., 2001. Enhanced short-term sediment deposition within the Nazaré canyon, north-east atlantic. Mar. Geol. 173, 55–67. https://doi.org/10.1016/S0025-3227(00)00163-8.
Settele, J., Scholes, R., Betts, R.A., Bunn, S., Leadley, P., Nepstad, D., Overpeck, J.T., Taboada, M.A., Fischlin, A., Moreno, J.M., Root, T., Musche, M., Winter, M., 2015. Terrestrial and inland water systems. Climate change 2014 impacts. Adaptation and Vulnerability: Part A: Global and Sectoral Aspects 271–360. https://doi.org/10.1017/CBO9781107415379.009.
Shafer, S.L., Bartlein, P.J., Anderson, K.H., Thompson, R.S., 2003. Assessment of Modern Climate Baselines for Paleoclimatic Reconstructions and Model Testing in North America., American Geophysical Union Fall Meeting. San Francisco, December 2003.
Silva, J.M.N., Moreno, M.V., Le Page, Y., Oom, D., Bistinas, I., Pereira, J.M.C., 2019. Spatiotemporal trends of area burnt in the Iberian Peninsula, 1975–2013. Reg. Environ. Change 19, 515–527. https://doi.org/10.1007/s10113-018-1415-6.
Smith, D.M., Griffin, J.J., Goldberg, E.D., 1973. Elemental carbon in marine sediments: a baseline for burning. Nature 241, 268–270. https://doi.org/10.1038/241268a0.
Sofiev, M., Siljamo, P., Ranta, H., Linkosalo, T., Jaeger, S., Rasmussen, A., Rantio-Lehtimaki, A., Severova, E., Kukkonen, J., 2013. A numerical model of birch pollen emission and dispersion in the atmosphere. Description of the emission module. Int. J. Biometeorol. 57, 45–58. https://doi.org/10.1007/s00484-012-0532-z.
Thevenon, F., Bard, E., Williamson, D., Beaufort, L., 2004. A biomass burning record from the West Equatorial Pacific over the last 360 ky: methodological, climatic and anthropic implications. Palaeogeography, Palaeoclimatology,. Palaeoecology 213, 83–99. https://doi.org/10.1016/S0031-0182(04)00364-5.
Tierney, J.E., Tingley, M.P., 2015. A TEX86 surface sediment database and extended Bayesian calibration. Sci Data 2 (150029). https://doi.org/10.1038/sdata.2015.29.
Tinner, W., Conedera, M., Ammann, B., Gaggeler, H.W., Gedye, S., Jones, R., Sagesser, B., 1998. Pollen and charcoal in lake sediments compared with historically documented forest fires in southern Switzerland since AD 1920. Holocene 8, 31–42. https://doi.org/10.1191/095968398667205430.
Trabaud, L., 1983. Evolution après incendie de la structure de quelques phytocénoses méditerranéennes du Bas-Languedoc (Sud de la France). Ann. For. Sci. 40, 177–196. https://doi.org/10.1051/forest:19830204.
Trigo, R.M., Sousa, P.M., Pereira, M.G., Rasilla, D., Gouveia, C.M., 2016. Modelling wildfire activity in Iberia with different atmospheric circulation weather types: modelling wildfire activity IN iberia. Int. J. Climatol. 36, 2761–2778. https://doi.org/10.1002/joc.3749.
Turco, M., von Hardenberg, J., AghaKouchak, A., Llasat, M.C., Provenzale, A., Trigo, R.M., 2017. On the key role of droughts in the dynamics of summer fires in Mediterranean Europe. Sci. Rep. 7 (81). https://doi.org/10.1038/s41598-017-00116-9.
Turner, R., Kelly, A., Roberts, N., 2004. A critical assessment and experimental comparison of microscopic charcoal extraction methods, in: proceedings of the Third International Meeting of Anthracology. pp. 265–272.
Turon, J.-L., 1984. Le Palynoplancton dans l'environnement actuel de l'Atlantique nord-oriental : évolution climatique et hydrologique depuis le dernier maximum glaciaire. Institut de géologie du bassin d'Aquitaine.
Umbanhowar, C.E., McGrath, M.J., 1998. Experimental production and analysis of microscopic charcoal from wood, leaves and grasses. Holocene 8, 341–346. https://doi.org/10.1191/095968398666496051.
Vale, C., Sundby, B., 1987. Suspended sediment fluctuations in the Tagus estuary on semi-diurnal and fortnightly time scales. Estuarine. Coastal and Shelf Science 25, 495–508. https://doi.org/10.1016/0272-7714(87)90110-7.
Vachula, R.S., 2021. A meta-analytical approach to understanding the charcoal source area problem. Palaeogeogr. Palaeoclimatol. Palaeoecol. 562, 110111. https://doi.org/10.1016/j.palaeo.2020.110111.
Vachula, R.S., Sae-Lim, J., Li, R., 2021. A critical appraisal of charcoal morphometry as a paleofire fuel type proxy. Quat. Sci. Rev. 262, 106979. https://doi.org/10.1016/j.quascirev.2021.106979.
Vale, C., Cortesão, C., Castro, O., Ferreira, A.M., 1993. Suspended-sediment response to pulses in river flow and semidiurnal and fortnightly tidal variations in a mesotidal estuary. Mar. Chem. 43, 21–31. https://doi.org/10.1016/0304-4203(93)90213-8.
Van der Weijden, C.H., Pacheco, F.A.L., 2006. Hydrogeochemistry in the Vouga river basin (central Portugal): pollution and chemical weathering. Appl. Geochem. 21, 580–613. https://doi.org/10.1016/j.apgeochem.2005.12.006.
van Weering, T.C.E., de Stigter, H.C., Boer, W., de Haas, H., 2002. Recent sediment transport and accumulation on the NW Iberian margin. Prog. Oceanogr. 52, 349–371. https://doi.org/10.1016/S0079-6611(02)00015-0.
Vazquez, A., Moreno, J., 1998. Patterns of lightning-, and people-caused fires in peninsular Spain. Int. J. Wildland Fire 8 (103). https://doi.org/10.1071/WF9980103.
Vázquez, A., Pérez, B., Fernández-González, F., Moreno, J.M., 2002. Recent fire regime characteristics and potential natural vegetation relationships in Spain. J. Veg. Sci. 13, 663–676. https://doi.org/10.1111/j.1654-1103.2002.tb02094.x.
Vázquez, J.T., Medialdea, T., Ercilla, G., Somoza, L., Estrada, F., Fernández Puga, M.C., Gallart, J., Gràcia, E., Maestro, A., Sayago, M., 2008. Cenozoic deformational structures on the Galicia bank region (NW iberian continental margin). Mar. Geol. 249, 128–149. https://doi.org/10.1016/j.margeo.2007.09.014.
Verardo, D.J., 1997. Charcoal analysis in marine sediments. Limnol. Oceanogr. 42, 192–197. https://doi.org/10.4319/lo.1997.42.1.0192.
Vernal, A., de Henry, M., Matthiessen, J., Mudie, P.J., Rochon, A., Boessenkool, K.P., Eynaud, F., GrØsfjeld, K., Guiot, J., Hamel, D., Harland, R., Head, M.J., Kunz-Pirrung, M., Levac, E., Loucheur, V., Peyron, O., Pospelova, V., Radi, T., Turon, J.-L., Voronina, E., 2001. Dinoflagellate cyst assemblages as tracers of sea-surface conditions in the northern North Atlantic, Arctic and sub-Arctic seas: the new ' $n = 677$' data base and its application for quantitative palaeoceanographic reconstruction: $n = 677$ CIRCUM-ARCTIC DINOFLAGELLATE CYST DATA BASE. J. Quat. Sci. 16, 681–698. https://doi.org/10.1002/jqs.659.
Villacieros-Robineau, N., Zúñiga, D., Barreiro-González, B., Alonso-Pérez, F., Granda, F., de la, Froján, M., Collins, C.A., Barton, E.D., Castro, C.G., 2019. Bottom boundary layer and particle dynamics in an upwelling affected continental margin (NW Iberia). J. Geophys. Res.: Oceans 124, 9531–9552. https://doi.org/10.1029/2019JC015619.
Whitlock, C., Larsen, C., 2002. Charcoal as a fire proxy. In: Smol, J.P., Birks, H.J.B., Last, W.M., Bradley, R.S., Alverson, K. (Eds.), Developments in Paleoenvironmental Research. Springer Netherlands Tracking Environmental Change Using Lake Sediments. Dordrecht, pp. 75–97. https://doi.org/10.1007/0-306-47668-1_5.